Becchimanzi *et al. Animal Microbiome* (2026) 8:13
https://doi.org/10.1186/s42523-025-00513-w

Animal Microbiome

RESEARCH Open Access

Deformed Wing Virus infection induces immunosuppression and gut dysbiosis in honey bees

Andrea Becchimanzi[1,2†], Giovanna De Leva[1†], Alfonso Cacace[1], Ilaria Di Lelio[1,2], Claudia Damiani[3], Maria Cristina Digilio[1,2], Emilio Caprio[1], Guido Favia[3] and Francesco Pennacchio[1,2*]

Abstract

Background The global decline of honey bee health, driven by multiple stressors impairing immunity, threatens both natural and managed ecosystems. Deformed Wing Virus (DWV) is often found at high loads in collapsing colonies, associated with an immunosuppressive syndrome still poorly understood. This study investigates gut microbiota community patterns associated with different levels of DWV infection, an overlooked aspect which can contribute to the reduction of immunocompetence in infected honey bees.

Results We quantified DWV in nurse bees from the field and compared gut microbiota in individuals with high vs. low viral loads. We also examined microbiota changes in bees experimentally infected with DWV. In both cases, highly infected bees showed a decreased transcription level of *dorsal 1-A*, a consolidated molecular proxy of reduced immunocompetence in honey bees. Host immunosuppression was associated with a consistent gut dysbiosis, marked by a reduced relative abundance of beneficial genera such as *Fructobacillus*, *Lactobacillus*, and *Apilactobacillus* (Firmicutes, Bacilli), and a relative enrichment of *Bartonella* (Proteobacteria).

Conclusions These findings shed new light on host-pathogen interactions and will allow a targeted manipulation of honey bee gut microbiota to limit DWV infections, which strongly contribute to colony losses.

Background

The decline in honey bee (*Apis mellifera*) health is a global concern with significant environmental and economic implications. Monitoring programs have reported substantial colony losses at local scales, with rates varying across countries and years [1–9]. In Italy, a mean colony loss of 17% was recorded in the winter of 2018–2019 [9], while in the USA, annual losses reached 60% in 2024–2025 [10]. The reduced survival of bee colonies results from a multifactorial syndrome driven by interacting stressors that collectively impair colony immunocompetence [11–13]. A common feature of collapsing colonies is the high prevalence of parasites and associated pathogens, particularly deformed wing virus (DWV)

†Andrea Becchimanzi and Giovanna De Leva co-first authors.

*Correspondence:
Francesco Pennacchio
f.pennacchio@unina.it
[1]Department of Agricultural Sciences, University of Napoli "Federico II", Napoli, Italy
[2]BAT Center - Interuniversity Center for Studies On Bioinspired Agro-Environmental Technology, University of Napoli "Federico II", Napoli, Italy
[3]School of Bioscience and Veterinary Medicine, University of Camerino, Camerino, Italy

[7, 14–16]. DWV (family Iflaviridae; genus *Iflavirus*) is an endemic immunosuppressive RNA virus of honey bees, vectored by the parasitic mite *Varroa destructor*, with which is symbiotically associated [17–20].

The mite *V. destructor* is an obligate ectoparasite of developing brood and adult honey bees, which feeds on host hemolymph and fat body [21–23]. This has a severe impact on host physiology, causing the reduction of weight and lifespan of adult bees [24–27] and the transmission of viral pathogens. Indeed, *V. destructor* acts as vector of several viruses, including acute bee paralysis virus (ABPV), Israeli acute paralysis virus (IAPV), black queen cell virus (BQCV) and Kashmir bee virus (KBV) [28]. However, the best known pathogen transmitted by *Varroa* mites is DWV, which causes the symptoms of crippled wings and shortened abdomens in individuals from heavily infested colonies [20, 29].

As the other viruses, DWV has been considered a minor problem to honey bee health before the occurrence of *Varroa* mites [30]. The vectoring activity and the immune stress caused by *V. destructor*, a relatively novel parasite for *A. mellifera*, promoted the spread and the uncontrolled replication of the virus, triggering the transition of common covert infections to devastating overt infections [18, 31, 32].

When transmitted by the mite or artificially injected, both widespread genotypes of DWV (A and B) act as highly virulent pathogens of *A. mellifera* [33–36]. The honey bee immune response is based on canonical immune pathways [37]. Although the primary antiviral defense response of honey bees is RNA interference (RNAi), other major immune pathways, such as Toll, IMD, and JACK/STAT, participate in antiviral response [38, 39]. Under limited stress conditions, DWV replication is controlled by the honey bee immune system, resulting in asymptomatic covert infections [38, 40–43]. However, increasing exposure to multiple stressors weakens antiviral defenses [12, 38], allowing uncontrolled viral replication [40, 41, 44]. This leads to a self-reinforcing cycle of immunosuppression, as increasing DWV titers further impair immune responses, primarily by targeting NF-κB signaling [12, 41]. Indeed, high viral levels are associated with a reduced expression of *dorsal-1 A* gene, which encode the NF-κB transcription factor involved in the response to several stressors, including pathogens [41, 42]. Dorsal is a key component of the Toll pathway, which regulates both systemic [17, 45] and gut immunity [46, 47] in honey bees. Gut immunity plays a crucial role in shaping the honey bee gut microbiota (GM), influencing both its composition and its ability to modulate immune responses at local [48, 49] and systemic levels [50], as observed in other model species [51]. Honey bee GM is a simple community dominated by 5 core species which are acquired after adult emergence through social interactions and contact with the hive environment [52, 53]. The core community, consistently found in healthy worker bees, comprises taxa within the genera *Bifidobacterium*, *Bombilactobacillus*, *Gilliamella*, *Lactobacillus*, and *Snodgrassella*. These species are functionally essential for host physiology, contributing to digestion, detoxification and immunity [52–56]. In addition to these core members, non-core but frequently detected taxa such as *Bartonella*, *Commensalibacter*, and *Frischella* may be present. Environmental (such as *Fructobacillus* spp.) or pathogenic bacteria (such as *Hafnia alvei*) are typically detected at low abundances in adult bee guts [57, 58]. Consequently, stressor-induced suppression of NF-κB signaling not only can directly compromise immunity but can also disrupt GM homeostasis, leading to a dysbiosis that could further weaken host immune defenses.

Here we focus on this hypothesis, by investigating GM community patterns associated with DWV infection by adopting a dual and complementary approach based on field-collected and artificially infected bees, analyzed via bacterial 16S rRNA amplicon sequencing and RT-qPCR. This approach highlights the central role of the GM as an interface between bees and their environment, where it may mediate and amplify synergistic interactions among multiple stressors, an aspect largely overlooked so far [12, 59]. Indeed, the GM of honey bees is susceptible to several perturbing factors, such as antibiotics [60], agrochemicals [61] and nutritional imbalances [62]. The possible consequences of gut dysbiosis, defined as an alteration in microbial balance and functionality in the gut, on bee health remain poorly understood [59]. However, considering that acute effects can range from reduced fitness of individuals [54] to dysfunctional social behavior [63, 64], the possible contribution of honey bee gut dysbiosis to colony collapse certainly warrants further investigation [65]. Recently, a study performed under controlled conditions indicated that dysbiotic honey bees are less tolerant to DWV infection than bees with a regular GM [66]. The present study, by investigating GM community patterns associated with DWV infection, will generate new information crucial for understanding the overall impact of this key viral pathogen on honey bee immunity and health. This will likely provide also useful insights on how to define targeted GM manipulations to alleviate the negative effects of one of the key stressors associated with honey bee colony losses worldwide.

Results

Characterization of DWV genotype landscape in field-collected and experimentally infected bees

To characterize the distribution of DWV genotypes in our honey bee colonies we quantified DWV-A and DWV-B loads in nurse bees collected over two consecutive years, as well as in bees experimentally infected with

a DWV lysate. In naturally infected nurse bees ($N = 100$), DWV-A and DWV-B loads showed a weak but positive correlation (Fig. 1a), suggesting only a limited degree of co-infection. Notably, DWV-A load was strongly correlated with total DWV load (Fig. 1b), whereas DWV-B showed only a weak correlation with total DWV load (Fig. 1c), indicating that DWV-A is the primary contributor to overall viral burden in these bees. Relative quantification revealed that DWV-A consistently dominated over DWV-B in field-collected bees, particularly at moderate to high infection levels (Fig. 1d). Interestingly, DWV-B represented a higher proportion of viral reads only in bees with extremely low total DWV loads (< 100 copies/ng RNA). When stratified by year, DWV-A remained significantly more abundant than DWV-B in both 2019 and 2020 (Fig. 1e), supporting the temporal stability of DWV-A dominance in natural infections. To assess genotype dynamics under controlled conditions, bees were injected with a DWV lysate obtained from symptomatic bees (i.e. bees with crippled wings indicating overt DWV infection). The viral lysate contained mostly DWV-A (1.60×10^4 copies/ng), which replicated to significantly higher levels than DWV-B in artificially infected bees (Fig. 1f–g). Non-injected control bees also harbored significantly more DWV-A than DWV-B, further reinforcing DWV-A's dominance. Together, these results confirm that DWV-A is the predominant circulating genotype in both natural and experimental conditions, and likely plays a central role in shaping viral dynamics in our experimental honey bee colonies.

Gut bacterial microbiota associated with DWV infection under natural conditions

Given the low abundance and weak correlation of DWV-B with overall viral load, we focused subsequent quantifications exclusively on DWV-A. This approach allows us to simplify the experimental design and data interpretation, while still capturing the main patterns of virus-host and virus-microbiota interactions relevant to honey bee health.

In a first set of observations, we compared GM composition of nurse bees with "low" (< 1 DWV copies/ng, $n = 7$) and "high" (> 10^5 DWV copies/ng, $n = 7$) DWV loads (Fig. 2a), the two extremes of the sampled population ($N = 58$). DWV-A load ranged from 0.23×10^1 to 3.90×10^6 viral genome copies in the carcasses obtained

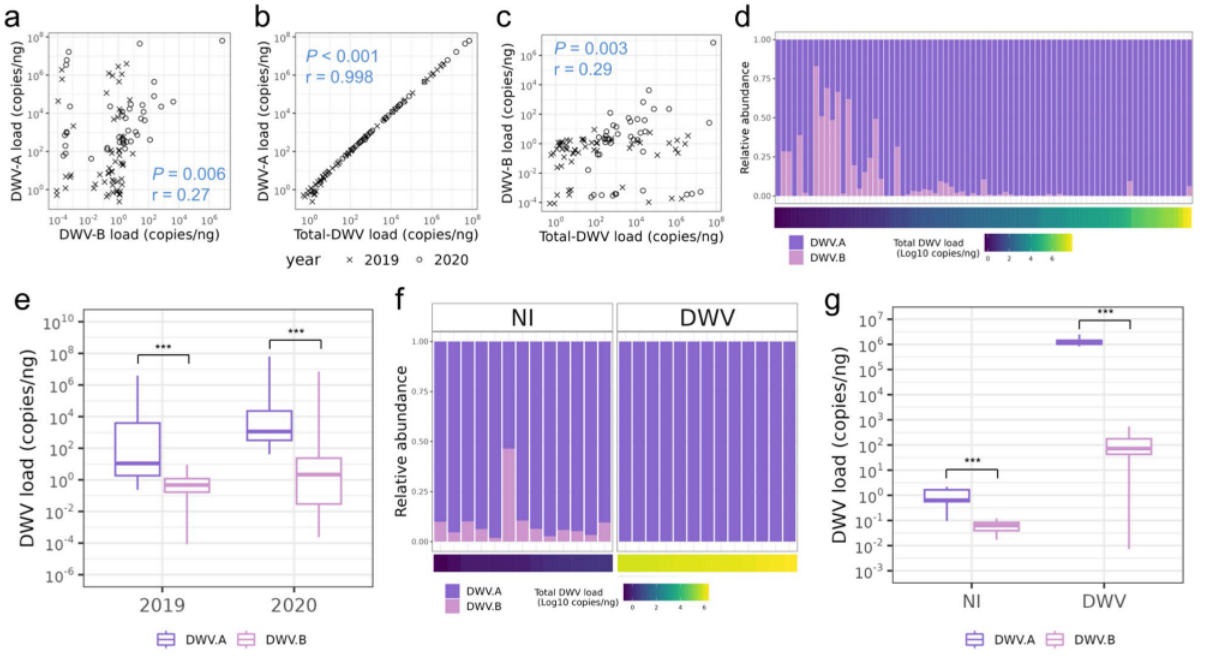

Fig. 1 Quantification of DWV genotype A and B in field-collected and lab-infected bees. (**a**) Loads of DWV-A and DWV-B were positively correlated in nurse bees collected over two consecutive years. (**b**) DWV-A load is strongly positively correlated with total DWV load in nurse bees. (**c**) DWV-B load is positively correlated with total DWV load in nurse bees. DWV load, normalized on total RNA extracted (copies/ng), was not normally distributed (Shapiro-Wilk test). In blue are indicated Spearman's rank correlation p-values (P) and rho (r). Nurse bees ($N = 100$) were field-collected over two consecutive years (2019–2020). (**d**) Relative abundance of DWV genotypes in field-collected (naturally infected) bees showed a dominance of DWV-A, except at low infection levels (0-100 copies/ng of RNA). (**e**) In both 2019 and 2020, DWV-A was significantly more abundant than DWV-B in naturally infected bees (Wilcoxon rank sum test, $P < 0.001$). (**f**) Relative abundance of DWV genotype in bees artificially infected (DWV) by injecting a viral lysate containing 1.60×10^4 DWV-A and < 2 DWV-B copies, compared with non-injected controls (NI). (**g**) In both non-injected (NI) and DWV-injected bees (DWV), DWV-A was significantly more abundant than DWV-B (Wilcoxon rank sum test, $P < 0.001$)

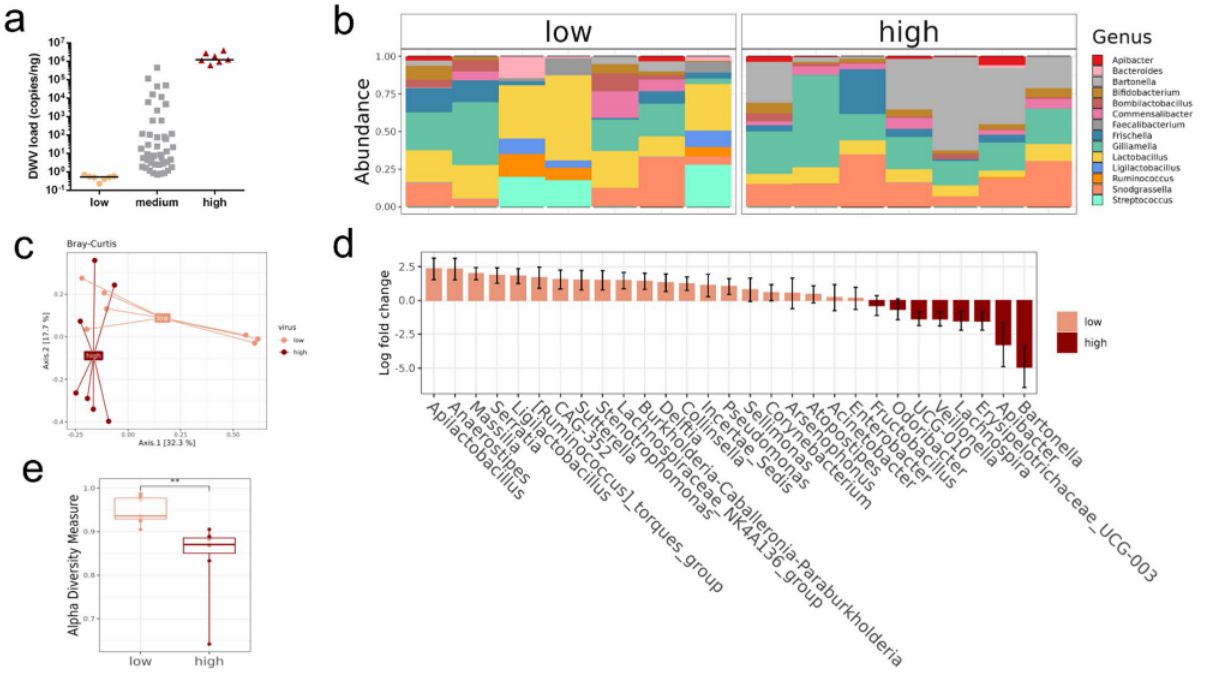

Fig. 2 Bacterial gut community of lowly and highly infected bees. (**a**) DWV loads of bees with "low" (< 1 DWV copies/ng) and "high" (> 10^5 DWV copies/ng) viral infection quantified by RT-qPCR. (**b**) Barchart of relative abundance at genus level. Each column represents a single sample. (**c**) Principal coordinate analysis of bacterial compositions per infection group based on Bray-Curtis dissimilarity matrix. Centroids are depicted as labels for low and high DWV groups. PERMANOVA indicated a significant difference between infection groups (F = 2.03, $P < 0.05$). (**d**) Significant ANCOM-BC results ($P < 0.05$) of genera associated with high and low DWV loads. (**e**) α-diversity (Simpson index) per infection group (Wilcoxon-test: W = 1, $P < 0.01$). Boxes denote inter-quartile range, bar denotes median, and whiskers denote range

after gut dissection. To identify differences in the abundance of core bacterial species between the two groups, DNA samples isolated from whole guts were used for bacterial profiling by 16 S rRNA sequencing.

Relative abundance composition revealed a different pattern in highly infected bees, characterized by an increased relative abundance of *Bartonella* (Alphaproteobacteria) and a relative reduction of *Lactobacillus* (Bacilli) (Fig. 2b and S1a). Notably, three samples in the lowly infected group were colonized by taxa which are not commonly associated with bees, such as *Ruminococcus*, *Ligilactobacillus* and *Streptococcus* (Fig. 2b). β-diversity analysis at the ASV level, based on Bray-Curtis dissimilarity matrix, revealed a significantly different composition between "low" and "high" groups (Fig. 2c; PERMANOVA: F = 2.03, $P < 0.05$). The most important contributors to these different compositions belong to the genus *Bartonella* and *Apilactobacillus*, associated with highly and lowly infected bees, respectively (ANCOM-BC; Fig. 2d). GM of highly infected bees showed a significant reduction of α-diversity, at the ASV level (Simpson Index; Fig. 2e; Wilcoxon-test: W = 1, $P < 0.01$).

In a second set of observations, we performed a hierarchical clustering based on β-diversity and, then, we compared viral loads between the clusters, to assess if different GM compositions were associated with different levels of DWV infection. DWV load in field-collected nurse bees, measured as DWV-A genome copies/ng of total RNA, ranged from 7.84×10^1 to 4.42×10^7 in 42 samples collected from two hives. All samples were processed for 16 S rRNA profiling and, after filtering for sequencing depth, the final dataset included 34 samples. Hierarchical clustering using Bray-Curtis dissimilarity and Ward's clustering algorithm identified two main biogroups (A and B) and five sub-groups (A1, A2, B1, B2, B3). The main groups A and B were associated with June and July sampling dates, respectively (Fig. 3a; X-squared = 7.63, df = 1, $P < 0.01$). DWV load was not different between A and B macro-groups, but it was higher in subgroups A1 and B2, compared to B3 and A2 (Fig. 3b). DWV load was not affected by hive (Fig. S2a) or by sampling date (Fig. S2b). No significant differences in α- or β-diversity were observed between colonies (Fig. S3a and S3b).

Our analysis reported the core bacterial genera of the honey bee adult microbiota. Barchart of relative abundance at genus level (Fig. 3c) showed that the biogroups with higher DWV loads, B2 and A1, are associated with higher abundance of *Bartonella* (Alphaproteobacteria, Fig. S1b). Differential abundance analysis indicated that *Bartonella* is significantly more abundant in nurse bees

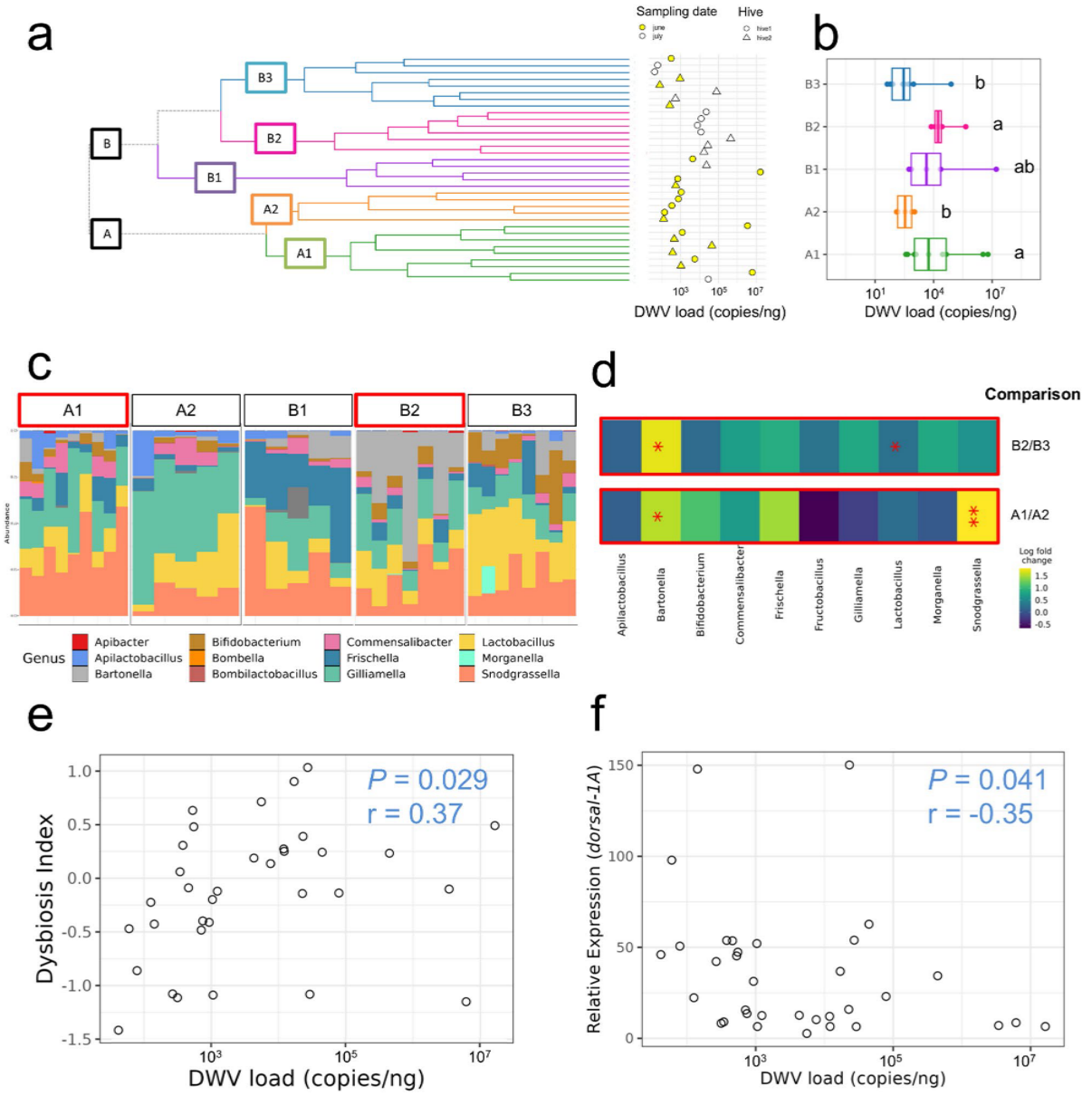

Fig. 3 Bacterial gut community associated with different DWV loads in nurse bees. (**a**) Hierarchical clustering, using Bray-Curtis distance (microbiota composition) and Ward's clustering algorithm, identified five biogroups and two main biogroups (A and B). These two latter, are associated with two different sampling dates (June and July), as indicated by Pearson's Chi-squared test (X-squared = 7.63, $P < 0.01$). (**b**) The five biogroups identified showed different viral levels, with A1 and B2 having higher DWV load than A2 and B3 (Kruskal-Wallis test = 14.6, df = 4, $P < 0.01$; Pairwise comparisons using Wilcoxon rank sum exact test with Benjamini-Hochberg correction). Biogroup B1 had an intermediate DWV load, compared to the other subgroups. (**c**) Barchart of relative abundance at genus level showed that biogroups with higher DWV loads, A1 and B2 (highlighted in red), are associated with a higher abundance of *Bartonella* (Alphaproteobacteria, gray). (**d**) Heatmaps showing differentially abundant genera identified by ANCOM-BC analysis. Compared to A2, A1 (higher DWV load, in the same macrogroup/period) showed a higher relative abundance of *Bartonella* and *Snodgrassella* (A1/A2). Compared to B3, B2 (higher DWV load, in the same macrogroup/period) showed higher relative abundance of *Bartonella*, and a reduced relative abundance of *Lactobacillus* (B2/B3). (**e**) Spearman correlations between DWV load and Dysbiosis Index (DI). DI, calculated using the formula: DI = log10((*Bartonella* abundance)/(*Lactobacillus* abundance)), was positively correlated with DWV load ($N = 34$). (**f**) DWV load correlated negatively with the expression of *dorsal-1 A*, a key gene of the immune response ($N = 34$). In blue are indicated Spearman's rank correlation p-values (P) and rho (r)

with higher DWV loads, such as A1 and B2 (Fig. 3d). On the other hand, *Lactobacillus* (Bacilli) was less abundant in one of the groups with higher DWV loads (B2), compared to B3 (Fig. 3d).

When testing these genera for correlation across all sampled nurse bees only *Bartonella* (Fig. S4a) and *Lactobacillus* (Fig. S4b) abundance resulted positively and negatively correlated with DWV load, respectively. Thus, we included both *Bartonella* and *Lactobacillus* abundance in a Dysbiosis Index (DI), which resulted positively correlated with DWV load (Fig. 3e). Moreover, as a proxy for measuring host immunocompetence we used the expression of a gene involved in the activation of the immune response, *dorsal-1 A* [41], which was negatively correlated with DWV load (Fig. 3f).

Effect of DWV artificial infection on bacterial GM

To demonstrate that the observed alterations of the GM associated with different levels of viral loads under field conditions are directly induced by different levels of DWV infection, we carried out a set of artificial infection experiments. We injected newly emerged individuals with a known quantity of DWV particles. To standardize their starting GM composition, we administered the same quantity of the same gut homogenate to all experimental individuals by one minute after virus injection. In the injected viral lysate DWV-B load was marginal compared to DWV-A load, representing only 0.003% of total DWV genome copies (Table S1). Indeed, honey bees receiving a viral lysate injection were prevalently infected by DWV-A genotype, 5 days after injection (Fig. 1f and g).

To assess any microbiota alteration induced by DWV infection we performed an experiment of artificial infection in which we compared gut bacterial community between DWV-injected (DWV) and PBS-injected bees (PBS) as control. This assay showed an increase of the relative abundance of *Bartonella* species in DWV-infected bees. The analyzed dataset included PBS ($n = 7$), with total DWV loads ranging from 4.34 to 20.6, and DWV bees ($n = 7$), with total DWV loads ranging from 3.39×10^7 to 1.67×10^8 copies per nanogram of total RNA (Fig. 4a). We scored the effect of artificial infection on the expression of *dorsal-1 A*, which was significantly reduced in DWV-injected bees (Fig. 4b), indicating the negative impact of viral infection on experimental bees. PERMANOVA revealed that gut community composition, at the ASV level, was significantly different between PBS and DWV (Fig. 4c). At the class level, members of the Alphaproteobacteria were more relatively abundant in DWV-injected bees compared with PBS (Fig. S1c, Wilcoxon-test: $W = 44$, $P < 0.05$). Relative abundance at the genus level showed a relative increase of *Bartonella* in the DWV group (Fig. 4d). However, these differences were not associated with a change of α-diversity in DWV-injected bees, at the ASV level (Simpson index, Fig. 4e). Differential abundance analysis identified *Bartonella* as the genus most differentially abundant in DWV-infected bees, compared to PBS-injected bees (ANCOM-BC, Fig. 4f). Moreover, Wilcoxon-test of relative abundances confirmed that *Bartonella* ($W = 47$, $P < 0.01$) was more abundant in DWV bees. Dysbiosis index comparison between groups showed a dysbiotic effect of DWV injection, compared to PBS (Fig. 4g).

To identify any GM change stably associated with DWV infection under a different experimental set-up, we compared DWV-injected bees with undisturbed bees (non-injected bees).The analyzed dataset included NI ($n = 13$), with total DWV loads ranging from 0.17 to 2.30, and DWV bees ($n = 13$), with total DWV loads ranging from 8.40×10^5 to 2.47×10^6 copies per nanogram of total RNA (approximately equal to 10^8-10^9 copies/bee) (Fig. 5a). We scored the effect of artificial infection on the expression of *dorsal-1 A*, which was significantly reduced in DWV bees (Fig. 5b). A total of 26 samples were sequenced generating an average of 389,906 reads per sample. The final table included 1483 ASVs. PERMANOVA at the ASV level revealed that gut community composition was significantly different between NI and DWV (Fig. 5c). At the class level, members of the Alphaproteobacteria were more relatively abundant in DWV-injected bees compared with NI (Wilcoxon-test: $W = 132$, $P = 0.014$), whereas Bacilli were more relatively abundant in NI bees (Wilcoxon-test: $W = 16$, $P < 0.001$) (Fig. S1d). Barplot at the genus level (Fig. 5d) showed a higher relative abundance of *Bartonella* and a relative reduction of *Lactobacillus* in DWV, compared to NI group. These differences were associated with a significant loss of α- in DWV-injected bees, at the ASV level (Simpson index, Fig. e). Differential abundance analysis identified gut bacterial taxa that differed in abundance between NI and DWV (Fig. 3f). Among bacterial genera associated with NI bees, *Lactobacillus* and *Fructobacillus* were those with the highest Log Fold-Change (LFC) values, while *Bartonella* and *Commensalibacter* were the most differentially abundant in DWV-infected bees (ANCOM-BC, Fig. 5f). Moreover, Wilcoxon-test of relative abundances confirmed that *Lactobacillus* ($W = 15$, $P < 0.001$) and *Fructobacillus* ($W = 8$, $P < 0.001$) were more abundant in NI, while *Bartonella* ($W = 143$, $P = 0.002$) and *Commensalibacter* ($W = 140$, $P = 0.003$) were more abundant in DWV bees. Dysbiosis index comparison between groups showed a marked dysbiotic effect of DWV injection (Fig. 5g). The relative abundance increase of the genus *Bartonella* appears to be consistently associated with DWV infection.

In a third experiment based on artificial infection, we scored the effect of DWV infection on GM in the

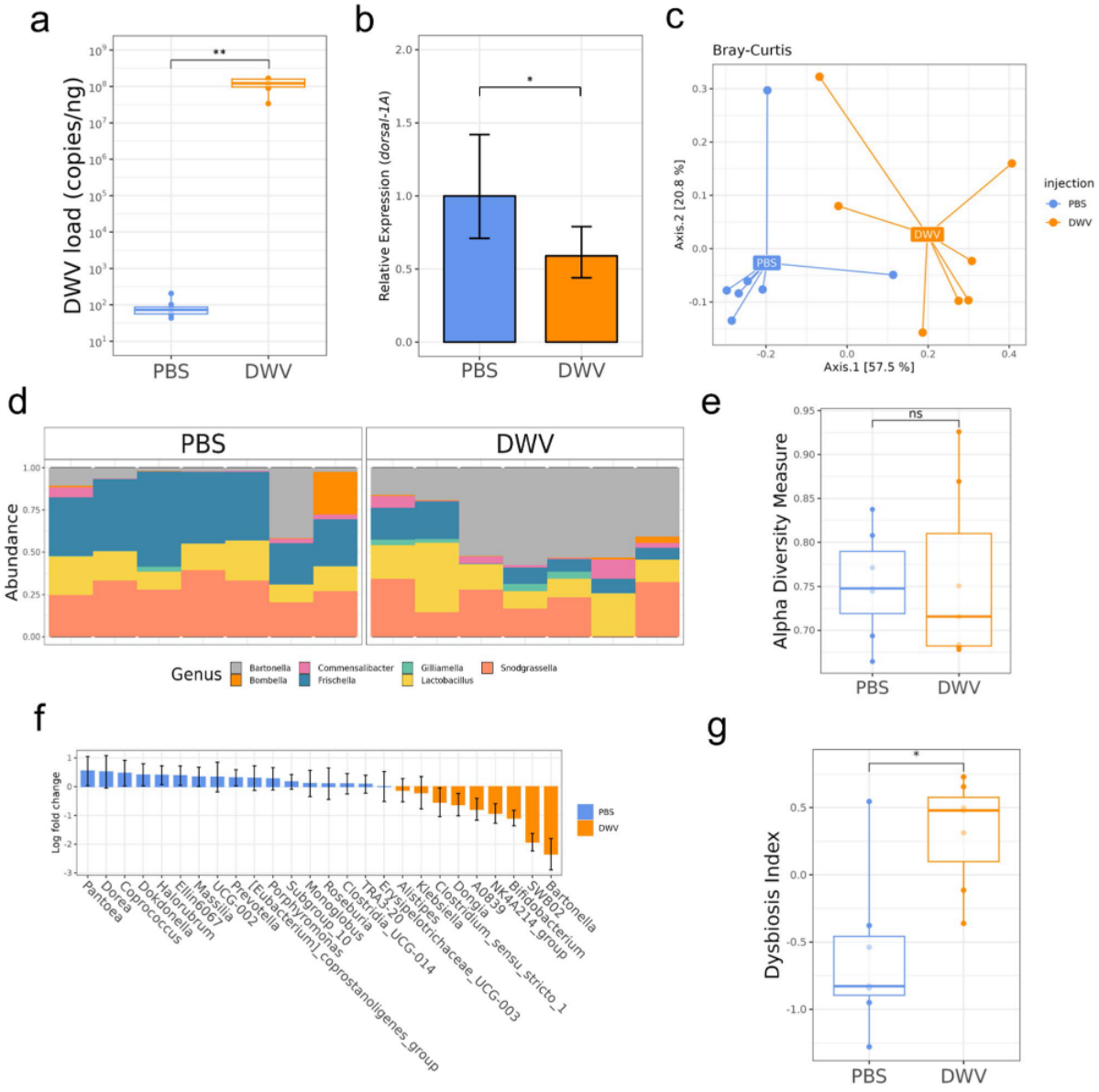

Fig. 4 Bacterial gut community of DWV-injected and PBS-injected bees in controlled conditions. (**a**) DWV load was significantly higher in DWV-injected (DWV, $n = 7$), compared to PBS-injected (PBS, $n = 7$) bees (Wilcoxon-test: $W = 49$, $P < 0.01$). (**b**) *Dorsal-1 A* expression was significantly lower in DWV bees, compared to PBS (Student's t-test: $t_{(11)} = 2.848$, $P < 0.05$). (**c**) Principal coordinate analysis of bacterial compositions per infection group. Centroids are depicted as labels for PBS and DWV groups. PERMANOVA indicated a significant difference between groups ($F_{(1, 12)} = 7.74$, $P < 0.01$). (**d**) Relative abundances at genus level. (**e**) α-diversity (Simpson index) per infection group. (**f**) Significant results of differential abundance analysis (ANCOM-BC; $P < 0.05$). (**g**) Dysbiosis index per infection group (Wilcoxon-test: $W = 44$, $P < 0.05$). Boxes denote inter-quartile range, bar denotes median, and whiskers denote range. ns = non-significant, *$P < 0.05$, **$P < 0.01$, ***$P < 0.001$, ****$P < 0.0001$

presence of the bacteria *Hafnia alvei*, to assess the impact of DWV-induced negative immunomodulation on the evolution of a background infection by an opportunistic pathogen. This experiment showed that DWV infection promoted the relative increase of *Hafnia*, along with the other opportunistic genera *Morganella* and *Klebsiella.* The analyzed dataset included PBS ($n = 7$), with total DWV loads ranging from 5.07×10^1 to 3.65×10^4, and DWV bees ($n = 7$), with total DWV loads ranging from 2.43×10^8 to 4.59×10^8 copies per nanogram of total RNA (Fig. 6a). The expression of *dorsal-1A* was significantly reduced in DWV bees (Fig. 6b). PERMANOVA at the ASV level revealed that gut community composition was significantly different between PBS and

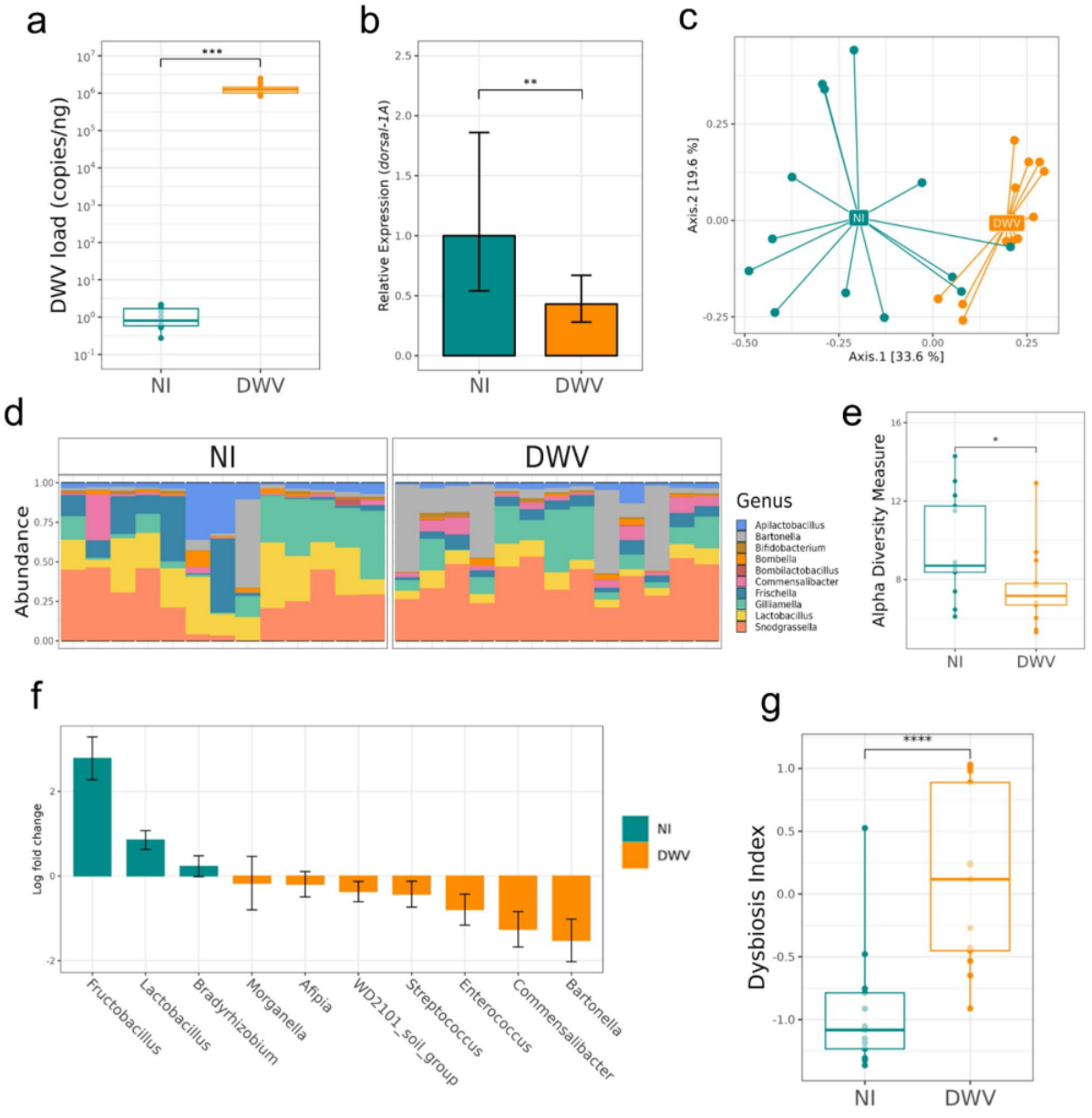

Fig. 5 Bacterial gut community of DWV-injected and non-injected bees under controlled conditions. (**a**) DWV load was significantly higher in DWV-injected (DWV, $n=13$), compared to non-injected (NI, $n=13$) bees (Wilcoxon-test: $W=0$, $P<0.0001$). (**b**) *Dorsal-1 A* expression was significantly lower in DWV infected bees, compared to NI (Student's t-test: $t_{(23.4)} = -4.07$, $P<0.001$). (**c**) Principal coordinate analysis of bacterial compositions per infection group. Centroids are depicted as labels for NI and DWV groups. PERMANOVA indicated a significant difference between groups ($F_{(1, 24)}=6.67$, $P<0.005$). (**d**) Relative abundances at genus level. (**e**) α-diversity (Simpson index) per infection group (Wilcoxon-test: $W=44$, $P<0.05$). (**f**) Significant results of differential abundance analysis (ANCOM-BC; $P<0.05$) included seven and three genera associated to DWV and NI, respectively. (**g**) Dysbiosis index per infection group (Wilcoxon-test: $W=155$, $P<0.0001$). Boxes denote inter-quartile range, bar denotes median, and whiskers denote range. *$P<0.05$, **$P<0.005$, ***$P<0.001$, ****$P<0.0001$

DWV treated bees (Fig. 6c). At the class level, members of the Gammaproteobacteria were more relatively abundant in DWV-injected bees compared with PBS (Fig. S1e, Wilcoxon-test: $W=45$, $P<0.01$). At the genus level, relative abundance of *Hafnia* was higher in DWV compared to PBS group (Fig. 6d). However, these differences were not associated with significant differences of α-diversity between the groups, at the ASV level (Simpson index, Fig. 6e). Differential abundance analysis identified *Morganella*, *Klebsiella* and *Hafnia* as the most differentially

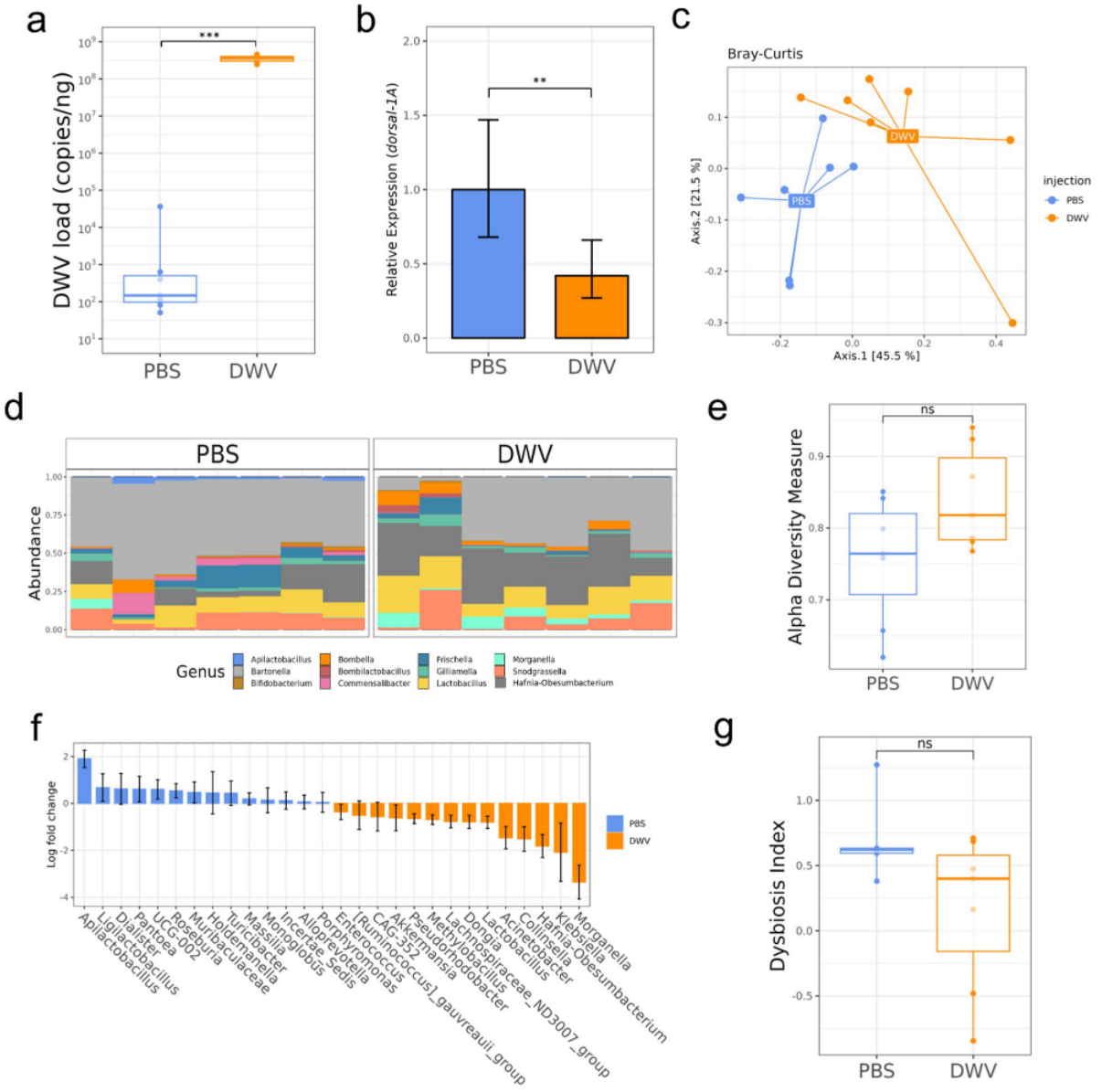

Fig. 6 Bacterial gut community of DWV-injected and PBS-injected bees naturally infected with *Hafnia alvei* in controlled conditions. (**a**) DWV load was significantly higher in DWV-injected (DWV, $n=7$), compared to PBS-injected (PBS, $n=7$) bees (Wilcoxon-test: $W=0$, $P<0.0001$). (**b**) *Dorsal-1 A* expression was significantly lower in DWV bees, compared to PBS (Student's t-test: $t_{(12)}=3.94$, $P<0.01$). (**c**) Principal coordinate analysis of bacterial compositions per infection group. Centroids are depicted as labels for PBS and DWV groups. PERMANOVA indicated a significant difference between groups ($F_{(1, 12)}=4.02$, $P<0.01$). (**d**) Relative abundances at genus level. (**e**) α-diversity (Simpson index) per infection group. (**f**) Significant results of differential abundance analysis (ANCOM-BC; $P<0.05$). (**g**) Dysbiosis index per infection group (Wilcoxon-test: $W=14$, $P=0.2$). Boxes denote inter-quartile range, bar denotes median, and whiskers denote range. ns = non-significant, $^{**}P<0.005$, $^{***}P<0.001$

abundant genera in DWV-infected bees, while *Apilactobacillus* was the most differentially abundant in PBS-injected bees (ANCOM-BC, Fig. 6f). Dysbiosis index, based on *Lactobacillus* and *Bartonella* abundance, did not differ between the experimental groups in presence of *Hafnia alvei* (Fig. 6g); this latter species was likely favored, along with other opportunistic pathogens, by DWV-induced immunosuppression.

Discussion

In this study, we investigated the impact of DWV infection on the honey bee GM using a combination of field sampling and controlled experimental infections. In a

first set of observations, involving nurse bees sampled during the summer, we characterized GM associated with different DWV levels, through 16 S rRNA sequencing. In complementary experiments, we corroborated our findings by artificially infecting bees with DWV and assessing their GM composition. This controlled setting allowed us to establish a causal relationship between DWV infection and microbiota changes.

Genotype-specific quantification of DWV revealed a higher load of DWV-A over DWV-B in nearly all bee samples, except for the lowest viral loads measured. This dominance of DWV-A over DWV-B genotype in our geographical context is confirmed by a recent study reporting 2017 data from the same locality [67], suggesting that our bees are still not affected by the global replacement of DWV-A by DWV-B [68].

In both field-sampled and artificially infected bees our study pointed out a negative correlation between DWV load and the expression of *dorsal-1 A*, a member of NF-kB family, playing a central role in the immune response [37]. This aligns with previous studies that have highlighted the immunosuppressive effects of DWV infection on honey bees [41, 42]. A recent study suggested that *dorsal-1 A* may participate in the regulation of Dual Oxidase (Duox) for ROS production in the honey bee gut, which acts as the effector in inhibiting non-native bacterial strains [47]. Therefore, the reduced expression of *dorsal-1 A* in response to DWV infection suggests a potential mechanism through which DWV can alter the GM composition, with a negative impact on immune competence, as a part of a complex virulence strategy.

Indeed, our microbial community analysis, based on Bray-Curtis dissimilarity, revealed significant differences in core GM composition between bees with different levels of DWV infection, in both field-sampled and artificially infected bees. In artificially infected bee experiments, PCA indicated a clear separation of gut community composition between infected and non-infected bees, despite all individuals received an equal dose of the same standardized gut homogenate, highlighting the potential impact of DWV infection on shaping the composition of the bacterial GM. This community shift is likely the result of an active DWV infection during microbiota colonization and establishment in the gut. The clustering of samples was more pronounced in the artificial infection experiments compared to field-collected bees, likely due to the controlled experimental conditions that minimized confounding factors such as bee age, which is known to influence microbiota composition [52, 69, 70]. Indeed, field sampling of honey bees inherently introduces age variability, which is a well-known challenge in microbiome studies of natural colonies [69, 71, 72]. This is also reflected in our first experiment comparing low- and high-DWV nurse bees. At the genus level, we observed unusually high relative abundances of taxa not typically associated with the honey bee core microbiota, such as *Ruminococcus*, *Streptococcus*, and *Ligilactobacillus*, in three out of seven lowly infected bees. Similar non-core or environmentally derived taxa have been documented in very young or recently emerged workers, whose gut communities are still assembling and remain highly sensitive to transient colonization [52, 53, 73]. Although we deliberately restricted sampling to nurse bees, this behavioral category spans individuals approximately 4–12 days old [74, 75]. It is therefore plausible that the low-DWV group included a subset of very young bees with immature microbiota, characterized by both lower stability and higher susceptibility to environmental microbes.

Another important source of variability of GM composition and viral susceptibility is represented by honey bee genetics [76–80]. However, our field observation indicated no differences between the two sampled hives in terms of DWV infection levels, α- and β-diversity. Future works will have to elucidate the influence of colony genetics on DWV-induced dysbiosis by including a larger number of colonies.

Importantly, this natural variability of field datasets was largely overcome in our controlled laboratory experiments, where both gut colonization and DWV infection occurred under standardized conditions. In these settings, a consistent pattern of DWV-associated microbiota alteration clearly emerged. Differential abundance analysis indicated that the observed compositional differences observed in our study are driven by a relative increase of *Bartonella* (Alphaproteobacteria) and a lower relative abundance of *Fructobacillus*, *Lactobacillus* and *Apilactobacillus* (Firmicutes, Bacilli). This pattern is characteristic of severe honey bee gut dysbiosis, which typically involves a drastic reduction in core taxa (e.g., Betaproteobacteria and Lactobacillus spp.) coupled with a bloom in other core species (e.g., Alphaproteobacteria and Gammaproteobacteria) [59, 60]. Similar dysbiotic shifts have been reported in response to xenobiotics, such as glyphosate, which depletes *Lactobacillus* species (*Lactobacillus* Firm-4 and Firm-5) within five days of exposure [61]. Nutritional stress is also a factor that can negatively impact gut microbial communities, leading to severe dysbiosis. For instance, a nutritionally poor-quality diet based on *Eucalyptus grandis* pollen was associated with reduced relative abundances of *Lactobacillus mellifer*, *Lactobacillus apis* (Firm-4 and Firm-5, respectively), and *Bifidobacterium* spp., along with an increased relative abundance of *Bartonella apis* [81], a compositional shift strikingly similar to our findings.

The artificially infected honey bees showed overall results consistent with what observed in field collected

material, with reduced *Lactobacillus* and increased *Bartonella* relative abundances; this latter shift appeared more consistently associated with DWV infection in the different experimental set-up considered. *Lactobacillus* species are well-known probiotics with potential applications in beekeeping [82], and their depletion in highly infected bees may indicate a protective role against DWV infection. Both *Fructobacillus* and *Apilactobacillus* are fructophilic lactic acid bacteria (FLAB), which thrive in D-fructose-rich niches, such as flowers, fruits and gastrointestinal tracts of insects [83–85]. FLABs display promising probiotic properties; for instance, *Fructobacillus pseudoficulneus* 57 stimulated immunity by up-regulating the expression of apidaecin, when administered to honey bee larvae [86]. Similarly, *Apilactobacillus kunkeei* EIR/BG-1, has shown a preventive effect against *Paenibacillus larvae* infection [87]. Additionally, a probiotic consortium comprising *Lactobacillus plantarum* Lp39, *Lactobacillus rhamnosus* GR-1, and *A. kunkeei* BR-1 (formerly *Lactobacillus kunkeei* BR-1), when administered via a nutrient patty, reduced pathogen load, upregulated key immune genes, and improved survival during *P. larvae* infection [88]. Considering that DWV tolerance can be promoted by honey bee GM [66], the use of lactic acid bacteria as probiotics against DWV infection represents a promising strategy for mitigating viral impact on honey bee colonies.

Our results raise interesting questions about the potential role of Alphaproteobacteria in modulating DWV infection. In particular, *Bartonella* [89] was associated to high DWV loads in both experiments. Interestingly, a capture-release study based on 14-day old adult bees from *Varroa*-resistant and -susceptible colonies in Gotland (Sweden) showed that *Bartonella apis* was consistently associated with colonies susceptible to *V. destructor* [90], the primary vector of DWV. The proliferation of *Bartonella* in honey bee gut has also been observed in wintering bees [72] and appears linked to its ability to utilize diverse energy substrates, such as metabolic waste products like lactate and ethanol [91], suggesting a sort of opportunistic behavior [65]. Such behavior is not surprising if we consider that *B. apis*, as well as the recently described *Bartonella choladocola* sp. nov. and *Bartonella apihabitans* [92], represents the closest relative of pathogenic *Bartonella* species [93]. Intriguingly, *B. choladocola* possesses genomic loci containing invasin and hemin-related genes, which may facilitate the invasion of gut barrier [92], suggesting that this species may both live as a gut symbiont and also as an opportunistic pathogen. This hypothesis is reinforced by our observation that relative increase of *Bartonella* abundance in both field-sampled and artificially infected bees correlates with reduced α-diversity, a hallmark of dysbiosis [60, 94–96]. This suggests a potential destabilizing effect of DWV infection on species richness and evenness in the gut, which promotes the proliferation of opportunistic species.

In the presence of the opportunistic bacterium *Hafnia alvei*, DWV-induced alterations of GM showed a different pattern of community shift, compared to our previous experiments. Specifically, DWV infection led to an increased relative abundance of *Hafnia* and other opportunistic genera (*Klebsiella* and *Morganella*), likely favored by the reduced immunocompetence of the host. Notably, in non-infected bees the most differentially abundant genus was *Apilactobacillus*, which has been shown to effectively control secondary infections by *Klebsiella* and *Morganella* [97]. Similarly, a recent study reported the reduction of *Lactobacillus apis* and the increase of opportunistic species (*Enterobacter* spp.) abundance in response to infection by chronic bee paralysis virus (CBPV), suggesting that microbiota dysregulation may be a common strategy employed by viral pathogens of honey bees to interfere with host immunity and facilitate infection [98].

It is interesting to note that the controlled laboratory experiments, even though limited to a single time point (5-day after infection) provide meaningful biological information. Indeed, the selected time point is relevant both for microbiota maturation and early viral effects. In honey bees, the gut microbiota typically reaches full colonization and stabilizes around 4–6 days after emergence [52], indicating that day 5 provides a reliable snapshot of the established community in young hive bees. Moreover, several studies show that gut bacterial communities can respond rapidly (within 2–5 days) to perturbations such as immune activation [50] or antibiotic exposure [99], suggesting that any impact by DWV infection on GM composition is detectable within this timeframe. DWV itself replicates quickly, with viral loads peaking around days 3–5 after infection [100]; thus, day 5 captures the window in which microbiota alteration is most likely evident. Nonetheless, while day 5 is appropriate for detecting early and biologically relevant shifts, longer-term longitudinal studies will be necessary to determine whether these changes persist or represent transient responses.

Moreover, because our findings are based on relative abundance profiles from amplicon sequencing, the observed increases or decreases in specific taxa reflect compositional shifts rather than absolute changes in bacterial load. While the overall trends we report are robust, we acknowledge that the underlying mechanisms cannot be fully resolved without absolute quantification of bacterial load (e.g., qPCR). Future studies incorporating extended time courses, multiple immune markers, absolute microbial quantification, and experimental manipulation of specific microbial taxa will be essential to

establish the sequentiality of functional changes underlying the host regulation strategy by DWV.

Despite these constraints, our results add a new piece of information to the complex network of functional interactions underlying the multifactorial regulation of honey bee health. Over the years, we have progressively integrated experimental evidence to refine a physiological model of honey bee immunosuppression by stress agents. Our previous studies first identified deformed wing virus (DWV) as a key driver of immunosuppression, a syndrome characterized by impaired NF-κB signaling [41]. This effect is further exacerbated by *Varroa destructor* infestation [17, 31, 101] and neonicotinoid insecticides [44, 102]. These findings underscore that any stressor engaging NF-κB, a central regulator of stress response, amplifies virus-induced immunosuppression. However, the precise mechanism by which DWV initiates and regulates this immunosuppressive state remains unclear. One possible mechanism of immunosuppression is mediated by the alteration of honey bees energy metabolism. Indeed, DWV coopts energy-related enzymes, particularly arginine kinase [103], likely impacting ATP turnover and possibly antiviral response mediated by K_{ATP} channels [104], although experimental validation is still required. This additional work, along with the research needs outlined above will help to clarify the directionality of the host regulation strategy: whether DWV infection actively drives gut dysbiosis, via immune system disruption, or whether the observed immunosuppression is the result of the gut dysbiosis.

In this study, we provide new insights on the impact of DWV infection on the gut microbiota, demonstrating that viral infection induces dysbiosis, a pattern commonly associated with immunosuppression and disease progression, as observed in other animal pathogens [105]. Furthermore, DWV-induced gut dysbiosis is expected to influence honey bee neurophysiology and behavior, given the emerging functional link between microbial metabolites, such as short-chain fatty acids produced by Firmicutes, and brain function [106, 107]. This mechanistic insight provides a strong rationale for the reported alleviation of viral infections through probiotic supplementation [66], as gut microbiota and systemic immunity are mutually regulated [50, 51]. These findings contribute to an emerging integrative framework, in which to place in-depth mechanistic studies required to develop more effective and targeted strategies to protect honey bee health.

Methods

Experimental design

Biological material

The honey bees used in this study were collected from *A. mellifera* colonies maintained at experimental apiary of the Department of Agricultural Sciences, University of Naples "Federico II". Colonies were regularly monitored for evaluating overall health conditions and treated against *Varroa* mites. The strength of bee colonies was estimated by checking the presence of an abundant population and provisions. All experiments were conducted during the warm season, from April to October.

Field observations

To investigate the relationships between DWV infection and the GM under natural conditions, two different sets of observations were carried out by collecting nurse bees, which are involved in maintaining the characteristic microbial community of the whole colony through constant contact with brood and trophallaxys [52]. Nurse bees, typically 4–12 days old [74, 75], were identified by observing their activity of nursing immatures on the frame. Asymptomatic individuals were collected by using a plastic tube and transported in a thermic bag. In the laboratory, they were immobilized by chilling, transferred in individual microcentrifuge tubes and stored at -20 °C.

In the first set of observations we collected 58 nurse bees from a single hive on a single date (July 2019), and quantified their DWV loads by RT-qPCR. Then, to assess if different infection levels are associated with different gut communities, we compared 16S profiles of the two extremes of our population, in terms of viral load: bees with lowest (< 1 DWV copies/ng; n = 7; "low";) and highest (> 10^5 DWV copies/ng; n = 7; "high") DWV titer. Notably, a threshold of 10^5 copies/ng RNA in the qPCR assay corresponds to approximately 10^8 viral copies per bee, which is considered a severe systemic infection in the literature and is associated with behavioral and immune alterations [17, 108–110]. In a second set of observations, 42 nurse bees were collected from two hives showing similar conditions of strength and provisions, in two sampling dates (9th June 2020 and 30th July 2020). In this case we followed a different strategy to assess if DWV is a possible contributor of gut community alterations: rather than labelling samples depending on their DWV load, we performed a hierarchical clustering based on β-diversity and then we compared viral loads between the clusters.

Laboratory experiments

To experimentally verify the possible effect of DWV infection on GM, we artificially infected newly emerged bees and maintained them under controlled conditions. To obtain adult bees, brood frames from a colony with no signs of DWV infection were brought into the laboratory and incubated in a dark chamber at 32 °C and 60% relative humidity overnight, from which bees eclosed naturally. Sampling dates are indicated in Table S4. Newly emerged bees were injected with a DWV lysate obtained

as described elsewhere [111]. Briefly, adult bees with symptomatic DWV infection (i.e. crippled wings) were homogenized in 500 µL 1X PBS in 1.5 mL microcentrifuge tubes. Tubes were centrifuged at 14,000 g for 10 min at 4°C and supernatant was clarified by adding an equal volume of chloroform. Samples were vortexed for 30 s, centrifuged at 10,000 g for 10 min at 4°C and supernatants were filtered through 0.22 µm sterile syringe filters (VWR, Radnor, Pennsylvania, USA). Lysates were stored in 40% glycerol at -80 °C until use. RNA isolated from a subsample of the viral lysates were evaluated for DWV load by qRT-PCR, as described below, and for the presence of other common bee viruses by PCR, as described elsewhere [112]. Newly emerged bees were cold-anesthetized at -20 °C for 3 min and then either injected (or not) with 2.5 µL of 1X PBS containing 10^4 DWV copies (or nothing), under a stereomicroscope (SteREO Discovery V8, Zeiss, Jena, Germany). Viral lysates were injected between 4th and 5^{ft} abdominal segments by using a beveled 33G NanoFil needle (NF33BV-2) mounted on a 10 µL NanoFil syringe (World Precision Instruments, Berlin, Germany). By one minute after injection, each bee was manually fed with 5 µL of honey bee gut homogenate, using a micropipette, to establish the characteristic gut community, as described elsewhere [50, 52, 66]. Briefly, to obtain freshly prepared gut homogenates, whole guts, dissected from four nurse bees, were homogenized in 500 µL 1X PBS and diluted 1:1 with 50% filtered sucrose/water solution. DWV-injected and control (PBS-injected or non-injected) bees were confined in separate disposable plastic cages (28 × 11 × 11 cm) and provided with pollen paste (90% w/w fresh corbicular pollen with water) and 50% filtered sucrose/water solution (w/v) *ad libitum*, inside an incubator at the abovementioned conditions. After 5 days, experimental bees were sampled and stored at -80 °C until dissection. The experiment was repeated three times: in the first we used non-injected bees as controls; in the second, we used PBS-injected bees as controls; in the third, we used PBS-injected bees as controls and collected the frame from a colony infested by *Hafnia alvei*, to score the effect of DWV under co-infection by an opportunistic gut pathogen. To detect colonies infected by *H. alvei*, we used specific PCR primers [113] on DNA extracted from a group of 20 hive bees. Adult bees used for the *H. alvei* experiment emerged with a high load of *H. alvei*, quantified through qPCR (Ct < 30) using a protocol described elsewhere [49].

Molecular analyses

Gut dissection and nucleic acids isolation

Sampled bees were pinned to a piece of styrophor with entomology pins and their abdomen was ventrally and sagittally cut using microforceps. The whole intestinal tract including crop, midgut, hindgut, and malpighian tubules was carefully removed using sterile forceps. Each gut sample was homogenized in 250µL of CTAB buffer (0.1 M Tris-HCl, pH 8; 1.4 M NaCl; 0.02 M EDTA, pH 8; 2% CTAB, w/v, 0.25% DTT, v/v, 50 µg/mL proteinase K) with a sterile plastic pestle and DNA was isolated as described elsewhere [114]. For each batch of DNA isolation, negative controls were performed to monitor for reagent and environmental contaminations: plastic pestles were immersed in the CTAB buffer without gut tissues, and samples were processed for DNA extraction as indicated above. The rest of the body of each bee (carcass) was individually placed in 250µL of TRIzol reagent (Thermo Fisher Scientific, Waltham, MA, USA) to isolate RNA, according to the manufacturer's instructions, for DWV quantification and gene expression analysis. The quantity and the quality of DNA and total RNA were assessed using Varioskan Flash spectrophotometer (Thermo Fisher Scientific).

Quantitative PCR to assess DWV loads and dorsal-1 A expression

The quantification of DWV genome copies in honey bee carcasses was performed using the Power SYBR Green RNA-to-Ct 1-Step Kit (Applied Biosystems) as described elsewhere [44]. All primers used are shown in Table S2. Titers of DWV-A and DWV-B were determined by relating the Ct values of unknown samples to an established standard curve. Each standard curve (Supplementary File 2) was established by plotting the logarithm of 10-fold dilutions of a starting solution containing 0.01 ng of purified PCR product (PureLink PCR Purification Kit, Thermo Fisher Scientific), against the corresponding Ct value as the average of three repetitions. Standard curves were constructed by using seven to ten dilution points per target (DWV-A, DWV-B), and the limit of detection corresponded to values of about 10^2 copies. The PCR efficiency was calculated based on the slope and coefficient of correlation (R^2) of the standard curve, according to the following formula: $E = 10^{(-1/\text{slope})} - 1$ (Table S3). DWV load was expressed as viral genome copies per nanogram of total RNA. Annealing temperature were set at 60 °C and 55 °C for DWV-A and DWV-B, respectively. A subset of the RNA samples extracted from carcasses of injected bees were tested for the presence of common honey bee viruses by PCR, including ABPV, CBPV, BQCV, KBV, SBV and DWV, as described elsewhere [112]. The results did not show any pathogenic viruses other than DWV.

Differential relative expression of *dorsal-1 A* was measured by one-step qRT-PCR, using the Power SYBR Green RNA-to-Ct 1-Step Kit (Applied Biosystems, Carlsbad, CA, USA), according to the manufacturer's instructions. Each reaction was prepared in 20 µL and contained 10 µL qRT-PCR mix 2X, 100 nM of forward and reverse primers, 0.16 µL of 125X RT enzyme mix, DEPC treated

water and 50 ng of total RNA. All samples were analyzed in duplicate on a Step One Real Time PCR System (Applied Biosystems). *β- actin* was used as endogenous control for RNA loading. Relative gene expression data were analyzed using the ΔΔCt method [115]. For validation of the ΔΔCt method, the difference between the Ct value of the target and the Ct value of *β-actin* transcripts [ΔCt = Ct(*dorsal-1 A*)-Ct (*β-actin*)] was plotted versus the log of ten-fold serial dilutions (100, 10, 1, 0.1 and 0.01 ng) of the purified RNA samples. The plot of log total RNA input versus ΔCt displayed a slope less than 0.1, indicating that the efficiencies of the two amplicons were approximately equal. The relative expression of *dorsal-1 A* in the control group was used as calibrator (relative expression = 1). The results are presented as mean fold changes.

16S rRNA sequencing and taxonomic annotation

The V3-V4 hypervariable region of the bacterial 16S rRNA gene was amplified using fusion primers with partial Illumina adaptors. The universal bacterial 341 F forward primer (5 -CCTACGGGNGGCWGCAG) and the 785R reverse primer (5 -GACTACHVGGGTATCTAATCC) were used. PCR reactions, library preparation and sequencing were performed by IGATech (Udine, Italy). Amplicons were paired-end sequenced (2 × 250 bp) on an Illumina NovaSeq 6000 platform using standard protocols. Raw fastq files were processed using the the QIIME2 platform [116]. The field conditions and artificial infection experiments were denoised and taxonomically annotated separately. For denoising and estimation of amplicon sequence variants (ASVs) in each samples, we used DADA2 algorithm [117] through QIIME2. Primers were trimmed while forward and reverse reads were not truncated. After training the naïve Bayes classifiers on SILVA reference sequences (SILVA release 138.1) [118], trimmed for the amplified region, the fit-classifier-sklearn method [119] was employed for the taxonomic annotation of the ASVs (confidence = 0.95).

Bioinformatic and statistical analyses

Diversity metrics and differential abundance

Subsequently, the ASVs assigned to mitochondria and chloroplasts were excluded, as well as the ASVs belonging to the most abundant genera identified in negative controls (pestle samples), including human/contaminants-associated taxa such as uncultured Caulobacteraceae, Burkholderiaceae, Sphingomonadaceae, Microbacteriaceae, *Cutibacterium*, *Nevskia*, *Variovorax*, *Ralstonia*, *Staphylococcus.* Subsequent analyses were performed using R packages 'phyloseq' and 'vegan'. Samples with less than 30,000 reads were excluded from the dataset. To plot relative abundances at class level, only taxa with more than 1% abundance in at least one sample were retained. Rarefaction curves were plotted (Fig. S5) to identify the optimal amount of reads to rarefy ASV tables (Table S4). Rarefied ASV tables were used as input for α- and β-diversity analyses. For α-diversity, we calculated the (Gini-) Simpson index using the 'estimate_richness' function, while for β-diversity we performed a principal coordinates analysis based on Bray-Curtis dissimilarity, using the 'ordinate' and 'distance' functions from 'phyloseq' package. To perform hierarchical clustering of samples based on community composition (Bray-Curtis distance), we used 'hclust' function with Ward's clustering algorithm [120]. Dendrograms were plotted using 'ggdendro' and 'ggplot' packages. To identify differentially abundant (DA) taxa, we used ANCOM-BC [121] with a significance thresholds of $P < 0.05$. To perform ANCOM-BC, rarefied table was used as input.

Dysbiosis index

The genera *Bartonella* and *Lactobacillus* identified as differentially abundant in the second field-collection experiment, were selected to test their correlation with DWV load, using Spearman's rank correlation. Significant correlations (positive for *Bartonella*, negative for *Lactobacillus*) were incorporated in a Dysbiosis Index (DI), to describe the dysbiotic status of each bees with a single value [94]. DI was calculated as the log ratio of geometric means of taxon absolute abundances that were positively correlated with DWV load (having $P < 0.05$ and $r > 0$) over taxa that were negatively correlated with DWV load (having $P < 0.05$ and $r < 0$).

$$DI \quad log_1 \quad \frac{\sqrt[n]{x_1\ x_2 \quad x_n}}{\overline{y_1\ y_2 \quad y}} \Bigg),$$

where each x denotes read counts for taxa positively correlated with DWV load and n is the total number of such taxa, whereas each y denotes read counts for taxa negatively correlated with DWV load and m is the total number of these taxa. Taxon read counts were used with an added pseudocount of 1, to accommodate the geometric mean by removing zeroes.

Statistical analyses

To analyze correlation between DWV infection and *dorsal-1 A* expression we used Spearman's rank correlation. Wilcoxon-test was used to test differences in α-diversity metric (inverse Simpson index), relative abundances (after centered log-ratio scale transformation) and DWV load of DWV-injected and non-injected bees. Student's t-test was used to analyze the effect of artificial infection on the expression of *dorsal-1 A*. The assumption of normal distribution of data was tested and met via Shapiro-Wilk test. Each dataset was checked for homoscedasticity using Levene's test. Community differences were verified

by permutational multivariate analysis of variance (PERMANOVA), using the 'adonis2' package. Pearson's Chi-squared test with Yates' continuity correction was used to assess if the main clusters identified by hierarchical clustering were associated with different hives or sampling dates. All statistical analyses were performed using R software, version 4.0.3.

Supplementary Information

The online version contains supplementary material available at https://doi.org/10.1186/s42523-025-00513-w.

Supplementary Material 1

Supplementary Material 2

Acknowledgements
We thank Prof. Francesco Nazzi (University of Udine, Italy) for providing a critical reading of an early draft of the manuscript.

Author contributions
Conceptualization & supervision: A.B., F.P.; Data acquisition: A.B., A.C., G.D.L., C.D.; Data analysis: A.B., G.D.L., I.D.L; Writing – original draft: A.B.; Writing – review & editing: M.C.D, E.C., F.P, G.F.

Funding
E.C. and F.P. were supported by the Ministry of University and Research (Italy) through the Projects of National Relevance (PRIN), grant no. P2022ZKPX3 (NEUROIMMUNITY), funded by the European Union – Next Generation EU, Mission 4 Component 1, CUP E53D23021100001 (https://www.mur.gov.it/). The funders had no role in study design, data collection and analysis, decision to publish, or preparation of the manuscript.

Data availability
Raw reads were deposited on the NCBI SRA database under the project accession PRJNA1287342.

Code availability
All scripts and datasets are deposited to Zenodo: https://doi.org/10.5281/zenodo.15915846.

Declarations

Ethics approval and consent to participate
Not applicable.

Competing interests
The authors declare no competing interests.

Received: 16 September 2025 / Accepted: 27 December 2025
Published online: 10 January 2026

References

1. Kulhanek K, Steinhauer N, Rennich K, Caron DM, Sagili RR, Pettis JS, et al. A National survey of managed honey bee 2015–2016 annual colony losses in the USA. J Apic Res. 2017;56:328–40. https://doi.org/10.1080/00218839.2017.1344496.
2. Porrini C, Mutinelli F, Bortolotti L, Granato A, Laurenson L, Roberts K, et al. The status of honey bee health in italy: results from the nationwide bee monitoring network. PLoS ONE. 2016;11:e0155411. https://doi.org/10.1371/journal.pone.0155411.
3. Ostroverkhova NV, Rosseykina SA, Yaltonskaya IA, Filinov MS. Estimates of the vitality and performances of apis mellifera mellifera and hybrid honey bee colonies in siberia: a 13-year study. PeerJ. 2024;12:e17354. https://doi.org/10.7717/peerj.17354.
4. Aurell D, Bruckner S, Wilson M, Steinhauer N, Williams GR. A National survey of managed honey bee colony losses in the USA: results from the bee informed partnership for 2020–21 and 2021–22. J Apic Res. 2024;63:1–14. https://doi.org/10.1080/00218839.2023.2264601.
5. Lee KV, Steinhauer N, Rennich K, Wilson ME, Tarpy DR, Caron DM, et al. A National survey of managed honey bee 2013–2014 annual colony losses in the USA. Apidologie. 2015;46:292–305.
6. van Engelsdorp D, Hayes J, Underwood RM, Pettis J. A survey of honey bee colony losses in the U.S., fall 2007 to spring 2008. PLoS ONE. 2008;3:e4071. https://doi.org/10.1371/journal.pone.0004071.
7. Genersch E, Von Der OHEW, Kaatz H, Schroeder A, Otten C, Büchler R, et al. The German bee monitoring project: a long term study to understand periodically high winter losses of honey bee colonies. Apidologie. 2010;41:332–52.
8. Gray A, Brodschneider R, Adjlane N, Ballis A, Brusbardis V, Charrière J-D, et al. Loss rates of honey bee colonies during winter 2017/18 in 36 countries participating in the COLOSS survey, including effects of forage sources. J Apic Res. 2019;58:479–85. https://doi.org/10.1080/00218839.2019.1615661.
9. Gray A, Adjlane N, Arab A, Ballis A, Brusbardis V, Charrière J-D, et al. Honey bee colony winter loss rates for 35 countries participating in the COLOSS survey for winter 2018–2019, and the effects of a new queen on the risk of colony winter loss. J Apic Res. 2020;59:744–51. https://doi.org/10.1080/00218839.2020.1797272.
10. Nearman A, Crawford CL, Guarna MM, Chakrabarti P, Lee K, Cook S, et al. Insights from U.S. Beekeeper triage surveys following unusually high honey bee colony losses 2024–2025. Sci Total Environ. 2025;1003:180650. https://doi.org/10.1016/j.scitotenv.2025.180650.
11. Neumann P, Carreck NL. Honey bee colony losses. J Apic Res. 2010;49:1–6.
12. Nazzi F, Pennacchio F. Disentangling multiple interactions in the hive ecosystem. Trends Parasitol. 2014;30:556–61. https://doi.org/10.1016/j.pt.2014.09.006.
13. Goulson D, Nicholls E, Botías C, Rotheray EL. Bee declines driven by combined stress from parasites, pesticides, and lack of flowers. Science. 2015;347:1255957.
14. Highfield AC, El Nagar A, Mackinder LCM, Noël LM-LJ, Hall MJ, Martin SJ, et al. Deformed wing virus implicated in overwintering honeybee colony losses. Appl Environ Microbiol. 2009;75:7212–20. https://doi.org/10.1128/AEM.02227-09.
15. Dainat B, Evans JD, Chen YP, Gauthier L, Neumann P. Predictive markers of honey bee colony collapse. PLoS ONE. 2012;7:e32151. https://doi.org/10.1371/journal.pone.0032151.
16. Kielmanowicz MG, Inberg A, Lerner IM, Golani Y, Brown N, Turner CL, et al. Prospective Large-Scale field study generates predictive model identifying major contributors to colony losses. PLoS Pathog. 2015;11:e1004816. https://doi.org/10.1371/journal.ppat.1004816.
17. Di Prisco G, Annoscia D, Margiotta M, Ferrara R, Varricchio P, Zanni V, et al. A mutualistic symbiosis between a parasitic mite and a pathogenic virus undermines honey bee immunity and health. PNAS. 2016;113:3203–8. https://doi.org/10.1073/pnas.1523515113.
18. Wilfert L, Long G, Leggett HC, Schmid-Hempel P, Butlin R, Martin SJM, et al. Deformed wing virus is a recent global epidemic in honeybees driven by Varroa mites. Science. 2016;351:594–7. https://doi.org/10.1126/science.aac9976.
19. Grozinger CM, Flenniken ML. Bee viruses: Ecology, Pathogenicity, and impacts. Ann Rev Entomol. 2019;64:205–26. https://doi.org/10.1146/annurev-ento-011118-111942.
20. de Miranda JR, Genersch E. Deformed wing virus. J Invertebr Pathol. 2010;103:S48–61. https://doi.org/10.1016/j.jip.2009.06.012.
21. Han B, Wu J, Wei Q, Liu F, Cui L, Rueppell O, et al. Life-history stage determines the diet of ectoparasitic mites on their honey bee hosts. Nat Commun. 2024;15:725. https://doi.org/10.1038/s41467-024-44915-x.
22. Ramsey SD, Ochoa R, Bauchan G, Gulbronson C, Mowery JD, Cohen A, et al. Varroa destructor feeds primarily on honey bee fat body tissue and not hemolymph. PNAS. 2019;116:1792–801. https://doi.org/10.1073/pnas.1818371116.
23. Rosenkranz P, Aumeier P, Ziegelmann B. Biology and control of Varroa destructor. J Invertebr Pathol. 2010;103(Suppl 1):S96–119. https://doi.org/10.1016/j.jip.2009.07.016.
24. De Jong D, De Jong PH, Gonçalves LS. Weight loss and other damage to developing worker honeybees from infestation with Varroa Jacobsoni. J Apic Res. 1982;21:165–7. https://doi.org/10.1080/00218839.1982.11100535.

25. Daly HV, Jong DD, Stone ND. Effect of parasitism by Varroa Jacobsoni on morphometrics of Africanized worker honeybees. J Apic Res. 1988;27:126–30. https://doi.org/10.1080/00218839.1988.11100791.
26. Bowen-Walker PL, Gunn A. The effect of the ectoparasitic mite, Varroa destructor on adult worker honeybee (Apis mellifera) emergence weights, water, protein, carbohydrate, and lipid levels. Entomol Exp Appl. 2001;101:207–17. https://doi.org/10.1046/j.1570-7458.2001.00905.x.
27. Annoscia D, Del Piccolo F, Nazzi F. How does the mite Varroa destructor kill the honeybee apis mellifera? Alteration of cuticular hydrcarbons and water loss in infested honeybees. J Insect Physiol. 2012;58:1548–55.
28. Tentcheva D, Gauthier L, Zappulla N, Dainat B, Cousserans F, Colin ME, et al. Prevalence and seasonal variations of six bee viruses in apis mellifera L. and Varroa destructor mite populations in France. Appl Environ Microbiol. 2004;70:7185–91. https://doi.org/10.1128/AEM.70.12.7185-7191.2004.
29. Boecking O, Genersch E. Varroosis – the ongoing crisis in bee keeping. J Verbr Lebensm. 2008;3:221–8. https://doi.org/10.1007/s00003-008-0331-y.
30. Bowen-walker PL, Martin SJ, Gunn A. The transmission of deformed wing virus between honeybees (*Apis mellifera* L.) by the ectoparasitic mite Varroa Jacobsoni Oud. J Invertebr. 1999;73–101.
31. Annoscia D, Brown SP, Di Prisco G, De Paoli E, Del Fabbro S, Frizzera D, et al. Haemolymph removal by Varroa mite destabilizes the dynamical interaction between immune effectors and virus in bees, as predicted by volterra's model. Proc Biol Sci. 2019;286:20190331. https://doi.org/10.1098/rspb.2019.0331.
32. Nazzi F, Le Conte Y. Ecology of Varroa destructor, the major ectoparasite of the Western honey Bee, apis mellifera. Ann Rev Entomol. 2016;61:417–32. https://doi.org/10.1146/annurev-ento-010715-023731.
33. McMahon DP, Natsopoulou ME, Doublet V, Fürst M, Weging S, Brown MJF, et al. Elevated virulence of an emerging viral genotype as a driver of honeybee loss. Proc Royal Soc B: Biol Sci. 2016;283:20160811. https://doi.org/10.1098/rspb.2016.0811.
34. Tehel A, Vu Q, Bigot D, Gogol-Döring A, Koch P, Jenkins C, et al. The two prevalent genotypes of an emerging infectious Disease, deformed wing Virus, cause equally low pupal mortality and equally high wing deformities in host honey bees. Viruses. 2019;11:114. https://doi.org/10.3390/v11020114.
35. Kevill JL, de Souza FS, Sharples C, Oliver R, Schroeder DC, Martin SJ. DWV-A lethal to honey bees (Apis mellifera): A colony level survey of DWV variants (A, B, and C) in England, Wales, and 32 States across the US. Viruses. 2019;11:426. https://doi.org/10.3390/v11050426.
36. Dubois E, Dardouri M, Schurr F, Cougoule N, Sircoulomb F, Thiéry R. Outcomes of honeybee pupae inoculated with deformed wing virus genotypes A and B. Apidologie. 2020;51:18–34. https://doi.org/10.1007/s13592-019-00701-z.
37. Evans JD, Aronstein K, Chen YP, Hetru C, Imler J-L, Jiang H, et al. Immune pathways and defence mechanisms in honey bees apis mellifera. Insect Mol Biol. 2006;15:645–56. https://doi.org/10.1111/j.1365-2583.2006.00682.x.
38. Brutscher LM, Daughenbaugh KF, Flenniken ML. Antiviral defense mechanisms in honey bees. Curr Opin Insect Sci. 2015;10:71–82. https://doi.org/10.1016/j.cois.2015.04.016.
39. McMenamin A, Daughenbaugh K, Parekh F, Pizzorno M, Flenniken M. Honey bee and bumble bee antiviral defense. Viruses. 2018;10:395. https://doi.org/10.3390/v10080395.
40. Nazzi F, Pennacchio F. Honey bee antiviral immune barriers as affected by multiple stress factors: A novel paradigm to interpret colony health decline and collapse. Viruses. 2018;10:159. https://doi.org/10.3390/v10040159.
41. Nazzi F, Brown SP, Annoscia D, Del Piccolo F, Di Prisco G, Varricchio P, et al. Synergistic parasite-pathogen interactions mediated by host immunity can drive the collapse of honeybee colonies. PLoS Pathog. 2012;8:e1002735. https://doi.org/10.1371/journal.ppat.1002735.
42. Barroso-Arévalo S, Vicente-Rubiano M, Puerta F, Molero F, Sánchez-Vizcaíno JM. Immune related genes as markers for monitoring health status of honey bee colonies. BMC Vet Res. 2019;15:72. https://doi.org/10.1186/s12917-019-1823-y.
43. Durand T, Bonjour-Dalmon A, Dubois E. Viral Co-Infections and antiviral immunity in honey bees. Viruses. 2023;15:1217. https://doi.org/10.3390/v15051217.
44. Annoscia D, Di Prisco G, Becchimanzi A, Caprio E, Frizzera D, Linguadoca A, et al. Neonicotinoid Clothianidin reduces honey bee immune response and contributes to Varroa mite proliferation. Nat Commun. 2020;11:5887. https://doi.org/10.1038/s41467-020-19715-8.
45. Lourenço AP, Florecki MM, Simões ZLP, Evans JD. Silencing of apis mellifera dorsal genes reveals their role in expression of the antimicrobial peptide defensin-1. Insect Mol Biol. 2018;27:577–89. https://doi.org/10.1111/imb.12498.
46. Chmiel JA, Daisley BA, Burton JP, Reid G. Deleterious effects of neonicotinoid pesticides on Drosophila melanogaster immune pathways. mBio. 2019;10. https://doi.org/10.1128/mBio.01395-19.
47. Guo L, Tang J, Tang M, Luo S, Zhou X. Reactive oxygen species are regulated by immune deficiency and toll pathways in determining the host specificity of honeybee gut bacteria. Proc Natl Acad Sci. 2023;120(e2219634120). https://doi.org/10.1073/pnas.2219634120.
48. Emery O, Schmidt K, Engel P. Immune system stimulation by the gut symbiont Frischella Perrara in the honey bee (Apis mellifera). Mol Ecol. 2017;26:2576–90. https://doi.org/10.1111/mec.14058.
49. Lang H, Duan H, Wang J, Zhang W, Guo J, Zhang X, et al. Specific strains of honeybee gut Lactobacillus stimulate host immune system to protect against pathogenic hafnia alvei. Microbiol Spectr. 2022;10:e0189621. https://doi.org/10.1128/spectrum.01896-21.
50. Kwong WK, Mancenido AL, Moran NA. Immune system stimulation by the native gut microbiota of honey bees. R Soc Open Sci. 2017;4:170003. https://doi.org/10.1098/rsos.170003.
51. Jordan CKI, Clarke TB. How does the microbiota control systemic innate immunity? Trends Immunol. 2024;45:94–102. https://doi.org/10.1016/j.it.2023.12.002.
52. Powell JE, Martinson VG, Urban-Mead K, Moran NA. Routes of acquisition of the gut microbiota of the honey bee apis mellifera. Appl Environ Microbiol. 2014;80:7378–87. https://doi.org/10.1128/AEM.01861-14.
53. Kwong WK, Moran NA. Gut microbial communities of social bees. Nat Rev Microbiol. 2016;14:374–84. https://doi.org/10.1038/nrmicro.2016.43.
54. Zheng H, Steele MI, Leonard SP, Motta EVS, Moran NA. Honey bees as models for gut microbiota research. Lab Anim. 2018;47:317–25. https://doi.org/10.1038/s41684-018-0173-x.
55. Engel P, Moran NA. The gut microbiota of insects – diversity in structure and function. FEMS Microbiol Rev. 2013;37:699–735. https://doi.org/10.1111/1574-6976.12025.
56. Bonilla-Rosso G, Engel P. Functional roles and metabolic niches in the honey bee gut microbiota. Curr Opin Microbiol. 2018;43:69–76. https://doi.org/10.1016/j.mib.2017.12.009.
57. Motta EVS, Moran NA. The honeybee microbiota and its impact on health and disease. Nat Rev Microbiol. 2024;22:122–37. https://doi.org/10.1038/s41579-023-00990-3.
58. Moran NA, Hansen AK, Powell JE, Sabree ZL. Distinctive gut microbiota of honey bees assessed using deep sampling from individual worker bees. PLoS ONE. 2012;7:e36393. https://doi.org/10.1371/journal.pone.0036393.
59. Daisley BA, Chmiel JA, Pitek AP, Thompson GJ, Reid G. Missing microbes in bees: how systematic depletion of key symbionts erodes immunity. Trends Microbiol. 2020;28:1010–21. https://doi.org/10.1016/j.tim.2020.06.006.
60. Raymann K, Shaffer Z, Moran NA. Antibiotic exposure perturbs the gut microbiota and elevates mortality in honeybees. PLoS Biol. 2017;15:e2001861. https://doi.org/10.1371/journal.pbio.2001861.
61. Motta EVS, Raymann K, Moran NA. Glyphosate perturbs the gut microbiota of honey bees. PNAS. 2018;115:10305–10. https://doi.org/10.1073/pnas.1803880115.
62. Maes PW, Rodrigues PAP, Oliver R, Mott BM, Anderson KE. Diet-related gut bacterial dysbiosis correlates with impaired development, increased mortality and Nosema disease in the honeybee (Apis mellifera). Mol Ecol. 2016;25:5439–50. https://doi.org/10.1111/mec.13862.
63. Vernier CL, Chin IM, Adu-Oppong B, Krupp JJ, Levine J, Dantas G, et al. The gut Microbiome defines social group membership in honey bee colonies. Sci Adv. 2020;6:eabd3431. https://doi.org/10.1126/sciadv.abd3431.
64. Liberti J, Kay T, Quinn A, Kesner L, Frank ET, Cabirol A, et al. The gut microbiota affects the social network of honeybees. Nat Ecol Evol. 2022;6:1471–9. https://doi.org/10.1038/s41559-022-01840-w.
65. Anderson KE, Ricigliano VA. Honey bee gut dysbiosis: a novel context of disease ecology. Curr Opin Insect Sci. 2017;22:125–32. https://doi.org/10.1016/j.cois.2017.05.020.
66. Dosch C, Manigk A, Streicher T, Tehel A, Paxton RJ, Tragust S. The gut microbiota can provide viral tolerance in the honey bee. Microorganisms. 2021;9:871. https://doi.org/10.3390/microorganisms9040871.
67. Sircoulomb F, Dubois E, Schurr F, Lucas P, Meixner M, Bertolotti A, et al. Genotype B of deformed wing virus and related Recombinant viruses become dominant in European honey bee colonies. Sci Rep. 2025;15:4804. https://doi.org/10.1038/s41598-025-86937-5.

68. Paxton RJ, Schäfer MO, Nazzi F, Zanni V, Annoscia D, Marroni F, et al. Epidemiology of a major honey bee pathogen, deformed wing virus: potential worldwide replacement of genotype A by genotype B. Int J Parasitology: Parasites Wildl. 2022;18:157–71. https://doi.org/10.1016/j.ijppaw.2022.04.013.
69. Hroncova Z, Havlik J, Killer J, Doskocil I, Tyl J, Kamler M, et al. Variation in honey bee gut microbial diversity affected by ontogenetic Stage, age and geographic location. PLoS ONE. 2015;10:e0118707. https://doi.org/10.1371/journal.pone.0118707.
70. Copeland DC, Maes PW, Mott BM, Anderson KE. Changes in gut microbiota and metabolism associated with phenotypic plasticity in the honey bee apis mellifera. Front Microbiol. 2022;13:1059001. https://doi.org/10.3389/fmicb.2022.1059001.
71. Anderson KE, Maes P. Social microbiota and social gland gene expression of worker honey bees by age and climate. Sci Rep. 2022;12:10690. https://doi.org/10.1038/s41598-022-14442-0.
72. Kešnerová L, Emery O, Troilo M, Liberti J, Erkosar B, Engel P. Gut microbiota structure differs between honeybees in winter and summer. ISME J. 2020;14:801–14. https://doi.org/10.1038/s41396-019-0568-8.
73. Kowallik V, Mikheyev AS. Honey bee larval and adult Microbiome life stages are effectively decoupled with vertical transmission overcoming early life perturbations. mBio. 2021;12:e02966–21. https://doi.org/10.1128/mBio.02966-21.
74. Seeley TD. Adaptive significance of the age polyethism schedule in honeybee colonies. Behav Ecol Sociobiol. 1982;11:287–93. https://doi.org/10.1007/BF00299306.
75. Johnson BR. Within-Nest Temporal polyethism in the honey bee. Behav Ecol Sociobiol. 2008;62:777–84.
76. Wu J, Lang H, Mu X, Zhang Z, Su Q, Hu X, et al. Honey bee genetics shape the strain-level structure of gut microbiota in social transmission. Microbiome. 2021;9:225. https://doi.org/10.1186/s40168-021-01174-y.
77. Penn HJ, Simone-Finstrom M, Lang S, Chen J, Healy K. Host genotype and tissue type determine DWV infection intensity. Front Insect Sci. 2021;1:756690. https://doi.org/10.3389/finsc.2021.756690.
78. Penn HJ, Simone-Finstrom MD, Chen Y, Healy KB. Honey bee genetic stock determines deformed wing virus symptom severity but not viral load or dissemination following pupal exposure. Front Genet. 2022;13. https://doi.org/10.3389/fgene.2022.909392.
79. Svobodová K, Maitre A, Obregón D, Wu-Chuang A, Thaduri S, Locke B, et al. Gut microbiota assembly of Gotland varroa-surviving honey bees excludes major viral pathogens. Microbiol Res. 2023;274:127418. https://doi.org/10.1016/j.micres.2023.127418.
80. Bridson C, Vellaniparambil L, Antwis RE, Müller W, Gilman RT, Rowntree JK. Genetic diversity of honeybee colonies predicts gut bacterial diversity of individual colony members. Environ Microbiol. 2022;24:5643–53. https://doi.org/10.1111/1462-2920.16150.
81. Castelli L, Branchiccela B, Garrido M, Invernizzi C, Porrini M, Romero H, et al. Impact of nutritional stress on honeybee gut Microbiota, Immunity, and Nosema Ceranae infection. Microb Ecol. 2020;80:908–19. https://doi.org/10.1007/s00248-020-01538-1.
82. Daisley BA, Pitek AP, Chmiel JA, Gibbons S, Chernyshova AM, Al KF, et al. Lactobacillus spp. Attenuate antibiotic-induced immune and microbiota dysregulation in honey bees. Commun Biol. 2020;3:1–13. https://doi.org/10.1038/s42003-020-01259-8.
83. Endo A, Irisawa T, Futagawa-Endo Y, Takano K, du Toit M, Okada S, et al. Characterization and emended description of Lactobacillus Kunkeei as a fructophilic lactic acid bacterium. Int J Syst Evol Microbiol. 2012;62:500–4. https://doi.org/10.1099/ijs.0.031054-0.
84. Endo A, Salminen S. Honeybees and beehives are rich sources for fructophilic lactic acid bacteria. Syst Appl Microbiol. 2013;36:444–8. https://doi.org/10.1016/j.syapm.2013.06.002.
85. Maeno S, Nishimura H, Tanizawa Y, Dicks L, Arita M, Endo A. Unique niche-specific adaptation of fructophilic lactic acid bacteria and proposal of three Apilactobacillus species as novel members of the group. BMC Microbiol. 2021;21:41. https://doi.org/10.1186/s12866-021-02101-9.
86. Janashia I, Alaux C. Specific immune stimulation by endogenous bacteria in honey bees (Hymenoptera: Apidae). J Econ Entomol. 2016;109:1474–7. https://doi.org/10.1093/jee/tow065.
87. Kiran F, Sevin S, Ceylan A. Biocontrol potential of Apilactobacillus Kunkeei EIR/BG-1 against infectious diseases in honey bees (Apis mellifera L). Vet Res Commun. 2023;47:753–65. https://doi.org/10.1007/s11259-022-10036-3.
88. Daisley BA, Pitek AP, Chmiel JA, Al KF, Chernyshova AM, Faragalla KM, et al. Novel probiotic approach to counter Paenibacillus larvae infection in honey bees. ISME J. 2020;14:476–91. https://doi.org/10.1038/s41396-019-0541-6.
89. Kešnerová L, Moritz R, Engel P. Bartonella apis sp. nov., a honey bee gut symbiont of the class Alphaproteobacteria. Int J Syst Evol MicroBiol. 2016;66:414–21. https://doi.org/10.1099/ijsem.0.000736.
90. Thaduri S, Marupakula S, Terenius O, Onorati P, Tellgren-Roth C, Locke B, et al. Global similarity, and some key differences, in the metagenomes of Swedish varroa-surviving and varroa-susceptible honeybees. Sci Rep. 2021;11:23214. https://doi.org/10.1038/s41598-021-02652-x.
91. Li C, Tang M, Li X, Zhou X. Community dynamics in structure and function of honey bee gut bacteria in response to winter dietary shift. mBio. 2022;13:e01131–22. https://doi.org/10.1128/mbio.01131-22.
92. Liu Y, Chen J, Lang H, Zheng H. Bartonella Choladocola sp. nov. And Bartonella apihabitans sp. nov., two novel species isolated from honey bee gut. Syst Appl Microbiol. 2022;45:126372. https://doi.org/10.1016/j.syapm.2022.126372.
93. Segers FH, Kešnerová L, Kosoy M, Engel P. Genomic changes associated with the evolutionary transition of an insect gut symbiont into a blood-borne pathogen. ISME J. 2017;11:1232–44. https://doi.org/10.1038/ismej.2016.201.
94. Vujkovic-Cvijin I, Sortino O, Verheij E, Sklar J, Wit FW, Kootstra NA, et al. HIV-associated gut dysbiosis is independent of sexual practice and correlates with noncommunicable diseases. Nat Commun. 2020;11:2448. https://doi.org/10.1038/s41467-020-16222-8.
95. Ye M-H, Fan S-H, Li X-Y, Tarequl IM, Yan C-X, Wei W-H, et al. Microbiota dysbiosis in honeybee (Apis mellifera L.) larvae infected with brood diseases and foraging bees exposed to agrochemicals. Royal Soc Open Sci. 2021;8:201805. https://doi.org/10.1098/rsos.201805.
96. Bernard-Raichon L, Venzon M, Klein J, Axelrad JE, Zhang C, Sullivan AP, et al. Gut Microbiome dysbiosis in antibiotic-treated COVID-19 patients is associated with microbial translocation and bacteremia. Nat Commun. 2022;13:5926. https://doi.org/10.1038/s41467-022-33395-6.
97. Kačániová M, Kunová S, Ivanišová E, Terentjeva M, Gasper J. Antimicrobial effect of Lactobacillus Kunkeei against pathogenic bacteria isolated from bees' gut. Sci PAPERS Anim Sci BIOTECHNOLOGIES. 2019;52:100–100.
98. Deng Y, Yang S, Zhang L, Chen C, Cheng X, Hou C. Chronic bee paralysis virus exploits host antimicrobial peptides and alters gut microbiota composition to facilitate viral infection. ISME J. 2024;18:wrae051. https://doi.org/10.1093/ismejo/wrae051.
99. Allen NO, Copeland DC, Mott BM, Erickson R, Anderson KE. Antibiotic treatment of honey bee colonies alters early gut Microbiome assembly and induces persistent dysbiosis in newly emerged workers. Sci Rep. 2025;15:29031. https://doi.org/10.1038/s41598-025-12823-9.
100. Prayugo V, Payne AN, Bonning BC, Dolezal AG. Infection timelines and co-infection effects of Israeli acute paralysis virus and deformed wing virus in the honey bee (*Apis mellifera*). J Invertebr Pathol. 2026;214:108484. https://doi.org/10.1016/j.jip.2025.108484.
101. Becchimanzi A, Tatè R, Campbell EM, Gigliotti S, Bowman AS, Pennacchio F. A salivary chitinase of Varroa destructor influences host immunity and mite's survival. PLoS Pathog. 2020;16:e1009075. https://doi.org/10.1371/journal.ppat.1009075.
102. Di Prisco G, Cavaliere V, Annoscia D, Varricchio P, Caprio E, Nazzi F, et al. Neonicotinoid Clothianidin adversely affects insect immunity and promotes replication of a viral pathogen in honey bees. Proc Natl Acad Sci. 2013;110:18466–71.
103. Becchimanzi A, De Leva G, Mattossovich R, Camerini S, Casella M, Jesu G, et al. Deformed wing virus coopts the host arginine kinase to enhance its fitness in honey bees (Apis mellifera). BMC Biol. 2025;23:12. https://doi.org/10.1186/s12915-025-02117-x.
104. Fellows CJ, Simone-Finstrom M, Anderson TD, Swale DR. Potassium ion channels as a molecular target to reduce virus infection and mortality of honey bee colonies. Virol J. 2023;20:134. https://doi.org/10.1186/s12985-023-02104-0.
105. Douglas AE. Fundamentals of microbiome science: how microbes shape animal biology. Princeton, NJ: Princeton University Press; 2018.
106. Liberti J, Engel P. The gut microbiota — brain axis of insects. Curr Opin Insect Sci. 2020;39:6–13. https://doi.org/10.1016/j.cois.2020.01.004.
107. Cabirol A, Moriano-Gutierrez S, Engel P. Neuroactive metabolites modulated by the gut microbiota in honey bees. Mol Microbiol. 2024;122:284–93. https://doi.org/10.1111/mmi.15167.

108. Koziy RV, Wood SC, Kozii IV, Van Rensburg CJ, Moshynskyy I, Dvylyuk I, et al. Deformed wing virus infection in honey bees (*Apis mellifera* L). Vet Pathol. 2019;56:636–41. https://doi.org/10.1177/0300985819834617.
109. Schurr F, Tison A, Militano L, Cheviron N, Sircoulomb F, Rivière M-P, et al. Validation of quantitative real-time RT-PCR assays for the detection of six honeybee viruses. J Virol Methods. 2019;270:70–8. https://doi.org/10.1016/j.jviromet.2019.04.020.
110. Kaku NG, Jankauski MA, Doyle BF, Collins CJ, Flenniken ML. Inapparent virus infections differentially affect honey bee flight. Sci Adv. 2025. https://doi.org/10.1126/sciadv.adw8382.
111. de Miranda JR, Bailey L, Ball BV, Blanchard P, Budge GE, Chejanovsky N, et al. Standard methods for virus research in apis mellifera. J Apic Res. 2013;52:1–56. https://doi.org/10.3896/IBRA.1.52.4.22.
112. Chen YP, Pettis JS, Collins A, Feldlaufer MF. Prevalence and transmission of honeybee viruses. Appl Environ Microbiol. 2006;72:606–11. https://doi.org/10.1128/AEM.72.1.606-611.2006.
113. Abbott SL, Moler S, Green N, Tran RK, Wainwright K, Janda JM. Clinical and laboratory diagnostic characteristics and cytotoxigenic potential of hafnia alvei and hafnia paralvei strains. J Clin Microbiol. 2011;49:3122. https://doi.org/10.1128/JCM.00866-11.
114. Evans JD, Schwarz RS, Chen YP, Budge G, Cornman RS, De la Rua P, et al. Standard methods for molecular research in apis mellifera. J Apic Res. 2013;52:1–54. https://doi.org/10.3896/IBRA.1.52.4.11.
115. Livak KJ, Schmittgen TD. Analysis of relative gene expression data using real-time quantitative PCR and the 2(-Delta delta C(T)) method. Methods. 2001;25:402–8. https://doi.org/10.1006/meth.2001.1262.
116. Bolyen E, Rideout JR, Dillon MR, Bokulich NA, Abnet CC, Al-Ghalith GA, et al. Reproducible, interactive, scalable and extensible Microbiome data science using QIIME 2. Nat Biotechnol. 2019;37:852–7. https://doi.org/10.1038/s41587-019-0209-9.
117. Callahan BJ, McMurdie PJ, Rosen MJ, Han AW, Johnson AJA, Holmes SP. DADA2: High-resolution sample inference from illumina amplicon data. Nat Methods. 2016;13:581–3. https://doi.org/10.1038/nmeth.3869.
118. Quast C, Pruesse E, Yilmaz P, Gerken J, Schweer T, Yarza P, et al. The SILVA ribosomal RNA gene database project: improved data processing and web-based tools. Nucleic Acids Res. 2013;41(Database issue):D590–6. https://doi.org/10.1093/nar/gks1219.
119. Bokulich NA, Dillon MR, Bolyen E, Kaehler BD, Huttley GA, Caporaso JG. q2-sample-classifier: machine-learning tools for Microbiome classification and regression. J Open Res Softw. 2018;3:934. https://doi.org/10.21105/joss.00934.
120. Sirisena KA, Daughney CJ, Moreau M, Sim DA, Lee CK, Cary SC, et al. Bacterial bioclusters relate to hydrochemistry in New Zealand groundwater. FEMS Microbiol Ecol. 2018;94. https://doi.org/10.1093/femsec/fiy170.
121. Lin H, Peddada SD. Analysis of compositions of microbiomes with bias correction. Nat Commun. 2020;11:3514. https://doi.org/10.1038/s41467-020-17041-7.

Publisher's note